2

CR-133962

D2-118463-1

THE ANALYSIS OF THE TRANSIENT
PRESSURE RESPONSE OF THE SHUTTLE
EPS-ECS CRYOGENIC TANKS WITH
EXTERNAL PRESSURIZATION SYSTEMS
- FINAL REPORT

THE *BOEING* COMPANY
HOUSTON, TEXAS

June 29, 1973

DOCUMENT NO.   D2-118463-1
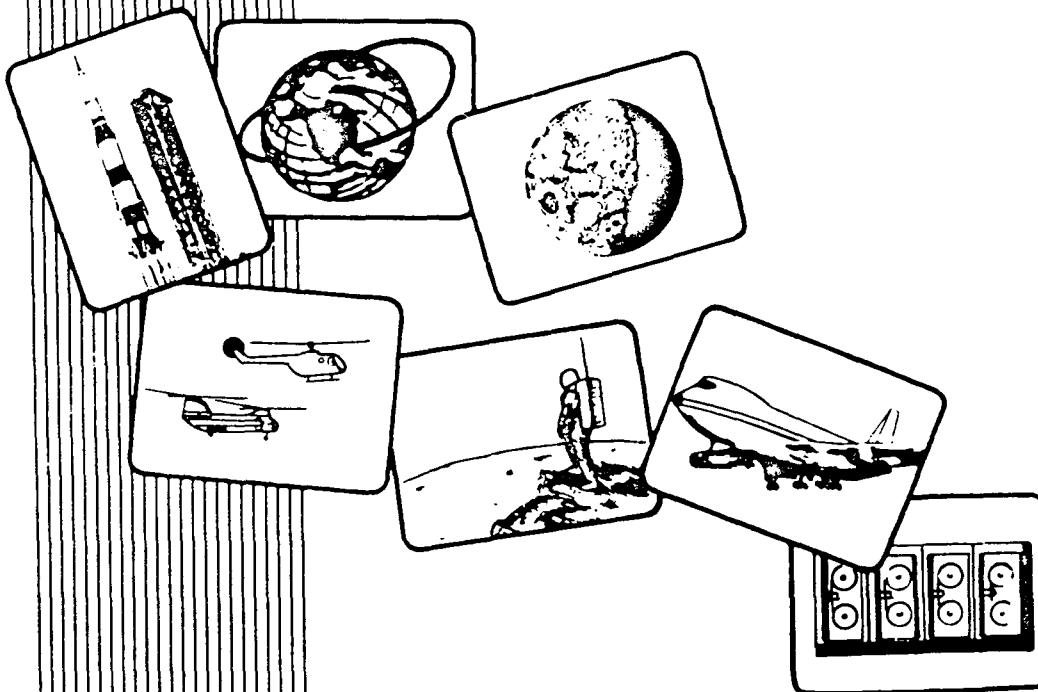

THE ANALYSIS OF THE TRANSIENT PRESSURE
TITLE   RESPONSE OF THE SHUTTLE EPS-ECS CRYOGENIC TANKS
WITH EXTERNAL PRESSURIZATION SYSTEMS - FINAL REPORT

CONTRACT NO.   NAS 9-12977

Prepared by:

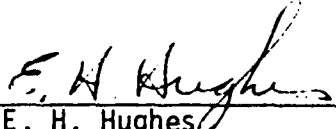Propulsion and Power Systems

Prepared for:

National Aeronautics and Space Administration
Lyndon B. Johnson Space Center
Houston, Texas

June 29, 1973

Prepared by: J. E. Barton
              H. W. Patterson

Approved by: _E. H. Hughes_____
              E. H. Hughes

BOEING AEROSPACE COMPANY, Houston, Texas

REVISIONS

REV. SYM	DESCRIPTION	DATE	APPROVED

ABSTRACT

An analysis of transient pressures in externally pressurized cryogenic hydrogen and oxygen tanks was conducted and the effects of design variables on pressure response determined. The analysis was conducted with a computer program which solves the compressible viscous flow equations in two-dimensional regions representing the tank and external loop. The external loop volume, thermal mass, and heat leak were the dominant design variables affecting the system pressure response. No significant temperature stratification occurred in the fluid contained in the tank.

KEY WORDS

Convection
Cryogenic
Heat Transfer
Pressure Cycles
Pressure Decay
Pressurization
Stratification
Thermodynamics

ACKNOWLEDGEMENTS

TABLE OF CONTENTS

ILLUSTRATIONS

ILLUSTRATIONS (continued)

REFERENCES

1. NASA JSC Contract NAS 9-12977, The Analysis of the Transient Pressure Response of the Shuttle EPS-ECS Cryogenic Tanks with External Pressurization Systems, dated June 21, 1972.

2. H. W. Patterson, C. K. Forester, and J. E. Barton, "Computer Program Manual Cryogenic Tank External Loop Pressurization Analysis," The Boeing Company, D2-118462-1.

3. J. E. Barton, G. I. Bultman, C. K. Forester, H. W. Patterson, D. D. Rule, and J. B. Urquhart, "Computer Program Manual Apollo Oxygen Tank Stratification Analysis Volume I of II," The Boeing Company, D2-118407-1A.

4. J. E. Barton, H. W. Patterson, and D. D. Rule, "Apollo Oxygen Tank Stratification Analysis Volume I of II," The Boeing Company, D2-118406-1.

5. H. Schlichting, Boundary Layer Theory.

SECTION 1

1.0 INTRODUCTION

1.1 PURPOSE

The primary purpose of the analysis of the Shuttle cryogenic tanks with external loop pressurization systems was to determine if pressure excursions resulting from loop operation could be satisfactorily controlled. Program objectives derived from this primary purpose were:

a. Develop a computer program to simulate transient pressures resulting from system operation in orbital flight environments.

b. Verify the accuracy of the computer program simulations as well as possible without actual system performance data.

c. Determine methods of controlling pressure excursions to acceptable limits by parametrically analyzing the effects of system design variables.

1.2 BACKGROUND

The Apollo cryogenic oxygen and hydrogen tanks were pressurized by internally installed electrical heaters. The limited maintainability of the internal heaters makes this system undesirable for the Shuttle application since reuseability is an operational requirement. An external loop pressurization system is being considered for the Shuttle application to provide improved maintainability. The transient performance characteristics of the internal system are well established from Apollo flight data and thermodynamic analyses. The transient pressure response of external loop pressurization systems in orbital environments has not been previously investigated. An analysis of the external pressurization system transient pressure response was needed to evaluate the system controllability in an orbital environment.

1.3 SCOPE

The analyses of external loop pressurization systems included detailed investigation of parameters which significantly affect the system transient pressure response. The analyses were not directed toward development of steady-state performance data. The analytical effort was divided into three tasks:

Task 1 - Model Development. Develop a computer program to simulate the tank transient pressure response.

Task 2 - Model Verification. Confirm the ability of the computer program to simulate physical phenomena which affect pressure response.

Task 3 - Parametric Data. Develop data required to determine the effect of loop design variables on the system transient pressures.

1.3 SCOPE (continued)

These three tasks are the complete effort initiated July 3, 1972 as defined in Contract NAS 9-12977, The Analysis of the Transient Pressure Response of the Shuttle EPS-ECS Cryogenic Tanks with External Pressurization Systems (Reference 1). The computer program resulting from Task 1 is described in the Computer Program Manual (Reference 2). The results of Task 2 and Task 3 are presented in this final report.

SECTION 2

2.0 SUMMARY

External loop pressurization systems are being considered for the Shuttle cryogenic tanks. External systems have a maintainability advantage over internal heaters used to pressurize the Apollo cryogenic tanks. Large pressure decays (greater than 100 psi) occurred in the Apollo oxygen tanks when fluid heated to high temperature near the heater was mixed with the cold bulk fluid. Similar pressure decays could occur with the external pressurization system due to temperature stratification in the tank and high temperature fluid in the loop. Analyses were needed to determine if external pressurization system design variables could be selected to limit pressure transients to acceptable values.

A computer program was developed to analyze the transient pressure response of cryogenic tanks with external loop pressurization systems. The computer program uses finite difference equations and techniques to simulate the fluid flow and heat transfer processes in the tank. The flow and heat transfer processes in the loop are treated using empirical heat transfer and pressure drop equations while the pump is on. When the pump is off, the loop analysis uses the same equations as used for the tank. Experimental pressurization system response data were not available for comparison with program simulation results. The program ability to analyze the tank flow field was satisfactorily verified by simulating a known laminar two-dimensional jet flow field. Verification of the thermodynamics calculations was not required since the same methods were successfully used to analyze Apollo tank performance.

Computer program simulations of oxygen and hydrogen pressure cycles indicated that loop volume, thermal mass, and heat leak significantly affected pressure transients. Other loop design variables had little effect on the system pressure response, and the fluid in the tank did not develop significant stratification. When the pump is turned on, a pressure drop occurs which is proportional to loop volume. A loop-to-tank volume ratio of .0004 limited the oxygen pressure drop to less than 22 psi. For hydrogen, a loop-to-tank volume ratio of .0003 resulted in approximately 2 psi pressure drop. Small pressure overshoots occurred in the hydrogen system after pump shutdown, but no overshoots were observed during oxygen simulations.

It was concluded from the analyses conducted that pressure transients can be adequately controlled by selection of the external loop design variables. The computer program developed for these analyses is adequate but should be verified with external loop pressurization system test data when available.

SECTION 3

3.0 PROGRAM TASKS

Three separate program tasks were established to determine the transient thermodynamic performance of the Shuttle supercritical cryogenic tanks. Program tasks necessary to achieve this objective were:

> Task 1 - Model Development
>
> Task 2 - Model Verification
>
> Task 3 - Parametric Data

The computer program resulting from Task 1 is described in detail by Reference 2. A general description of the computer program is included in this section. The significant results of Task 2 and Task 3 are also contained in this section.

3.1 TASK 1 - MODEL DEVELOPMENT

The computer program for the transient performance analysis of the external loop pressurization system simulates four major system components. The essential system elements are the tank, the pump, the line from the tank to the pump, and the line from the pump to the tank (Figure 3-1). The "external loop" includes the two lines and the pump. The computer program executive provides the interface between the loop and tank models and controls the loop on-off cycles based on system pressure.

3.1.1 Tank Model

The tank model was derived from the computer program developed under Contract NAS 9-11576 to analyze stratification in the Apollo oxygen tanks (Reference 3). The tank model treats the tank as a two-dimensional rectangular (X-Y coordinates) region as did the stratification model. Changes were made to the stratification model to improve the capability to analyze a tank with fluid injection from an external loop.

The model solves the partial differential equations for the conservation of mass, momentum, and energy using finite difference approximations. The stratification model solved the same equations but did not exactly conserve momentum due to the differencing method used. Momentum conservation was required to assure valid simulation of the tank response with cyclic injection of fluid from the external loop. If momentum were not conserved, the decay of fluid motion during the pump off periods would be unrealistic and could affect the fluid temperature distribution and pressure.

Momentum is conserved in the tank model by the revised difference equations used. The stratification model used donor cell or up-wind differences for the momentum convection terms (terms not involving viscosity). The donor cell difference method caused some loss in momentum each time step. The

LINE 2 (1x3 GRID)

TO TANK ← FROM PUMP

HEATER

FROM LINE 2

LINE OF SYMMETRY

TANK MODEL
(8x10 GRID)

TO LINE 2

PUMP

FROM
LINE 1

← INDICATES FLUID FLOW
DURING PUMP OPERATION

DEMAND FLOW
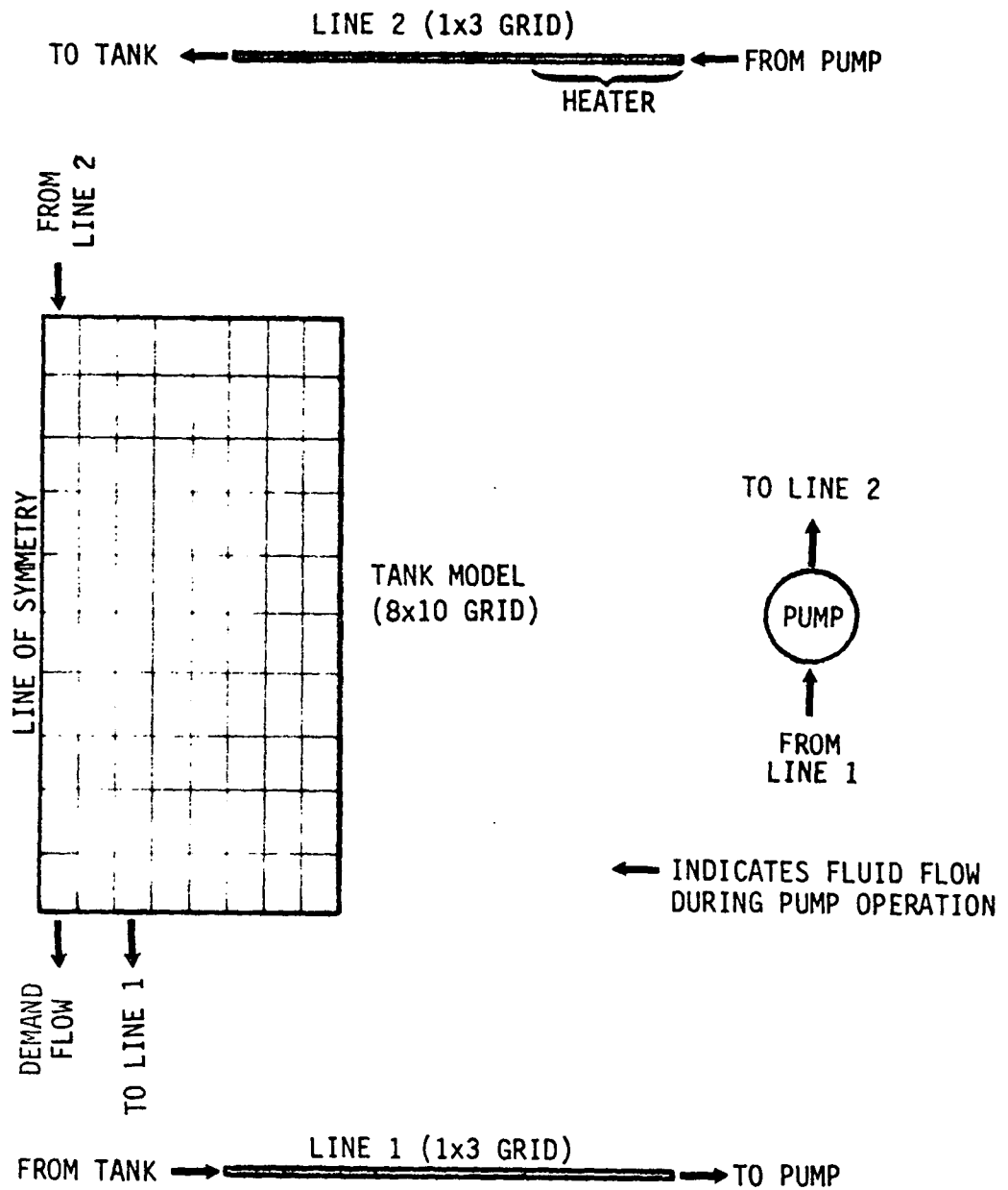
TO LINE 1

LINE 1 (1x3 GRID)

FROM TANK → → TO PUMP

FIGURE 3-1. MATH MODEL COMPONENT GRID DISTRIBUTION

3.1.1 Tank Model (continued)

revised difference equations use space and time centered differences for momentum convection. The space centering is necessary for momentum conservation, and time centering is required for stability of the solution. Time centering requires iteration to obtain values for the derivatives which are consistent with the current and forward time plane values. The viscous terms are not time centered since these terms do not contribute any artificial momentum loss and do not cause instability.

The tank model is also used to simulate the fluid in the lines while the pump is off. This application required adding a capability to analyze heat from the environment and the heat conducted along the line. These effects were included in the "heater" located on the left boundary of the two-dimensional region. Both radiation and conduction from an arbitrary environmental temperature are used to compute the heat input to the heater. The "heater" is used to represent the entire line wall, and electrical power input is specified for only cells representing the actual heater or heat exchanger.

Additional boundary conditions of the tank model were developed to provide the loop interface. One cell at the top of the rectangular region was modified to accept flow from the loop. One cell at the bottom provides the design outflow, and one nearby cell provides flow to the external loop. This modification requires specification of the enthalpy at the incoming flow in the dummy cell adjacent to the border. The capability for calculating the flow rate from the pressure change rate was also included. For this calculation, the flow rate for two of the three cells must be specified.

3.1.2 Loop Model

The external loop model treats the pump on and pump off periods by two different methods. While the pump is off, each of the lines is simulated using the tank model with appropriate boundary conditions. During this part of the pressure cycle, the flow rates in the lines are determined from thermodynamics only. When the pump is on, the flow rates are determined from line pressure drop, pump performance, and fluid thermodynamics. The program executive controls the transfer between the two calculation procedures.

During pump off periods, the loop is treated as two separate lines. Each line receives heat from the environment and expels fluid into the tank. The fluid expelled from the line into the tank is affected by the system pressure change rate. The tank model option to compute flow rate from pressure change rate is therefore used to analyze the lines for these conditions. Since the line volumes are small in comparison with the tank, the line pressures are slaved to the tank pressure which is considered as the system pressure.

During pump on periods, the loop flows are determined by the pump performance and the line pressure drop. The pump pressure rise is computed in the program as a cubic function of flow rate.

3.1.2 Loop Model (continued)

$$\frac{\Delta P}{\rho} \left(\frac{N_D}{N}\right)^2 = \sum_{I=1}^{4} A(I) \left(Q \cdot \frac{N_D}{N}\right)^{I-1}$$

where

ΔP = Pressure rise across pump (psi)

ρ = Density of incoming fluid (lbs/ft^3)

Q = Volumetric flow rate (ft^3/sec)

N_D = Pump design speed (rpm)

N = Pump speed (rpm)

$A(1)$ = .56708

$A(2)$ = 1.8025

$A(3)$ = -27.886

$A(4)$ = 46.235

The pressure rise equation was derived to represent the Airesearch pump developed for the Apollo program and tested at NASA JSC. The curve represented by the cubic equation is compared with the test data by Figure 3-2. The pump normalized efficiency is computed from the pressure rise equation by dividing the fluid power output by the maximum fluid power output (Figure 3-3). The product of the design efficiency and normalized efficiency are used to compute heat input to the fluid from the fluid power.

The line pressure drop is computed from the Blasius friction factor

$$f = \frac{.0791}{(R_e)^{\frac{1}{4}}}$$

where f is the friction factor and R_e is the Reynolds Number. The heat transfer from the line to the fluid is computed from the Sieder-Tate relationship

$$Q = K(\Delta L)(\Delta T)(R_e)^{.8}(P_R)^{1/3}\left(\frac{\mu}{\mu_W}\right)^{.14}(.026)(3.1416)$$

where

Q = Heat transfer

K = Fluid conductivity

ΔL = Length
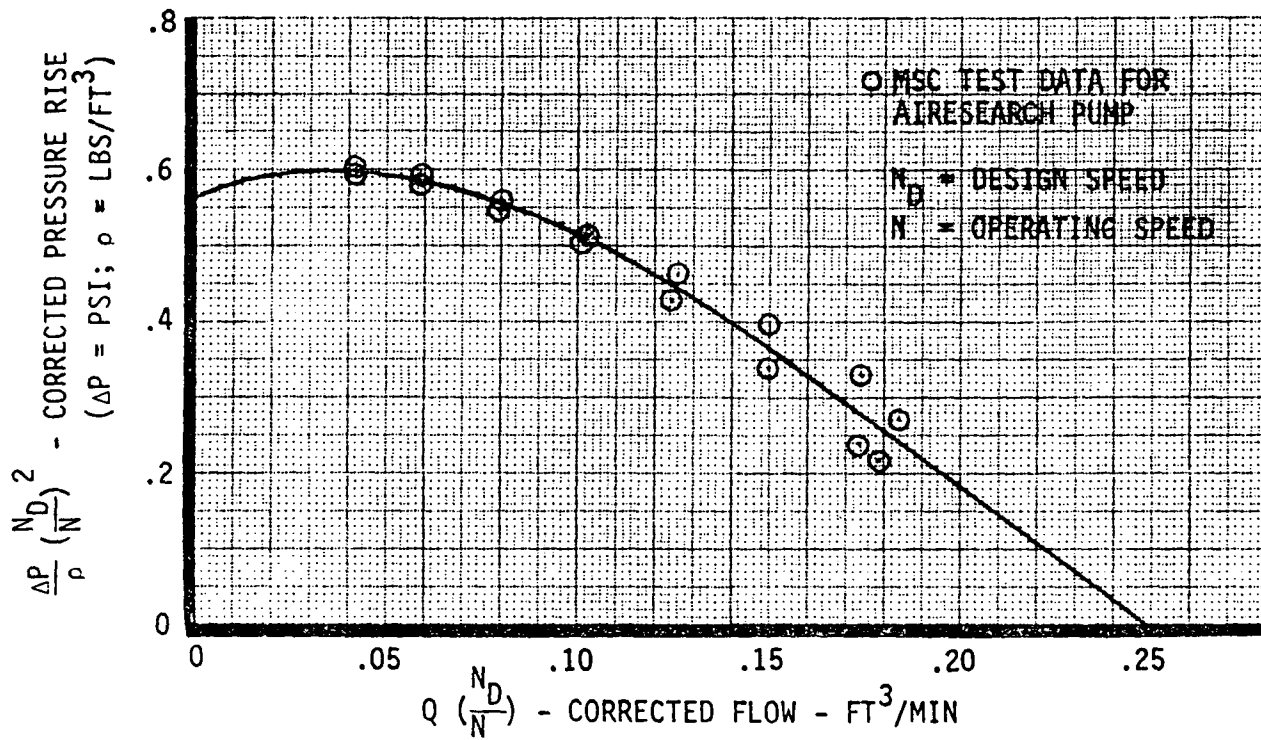
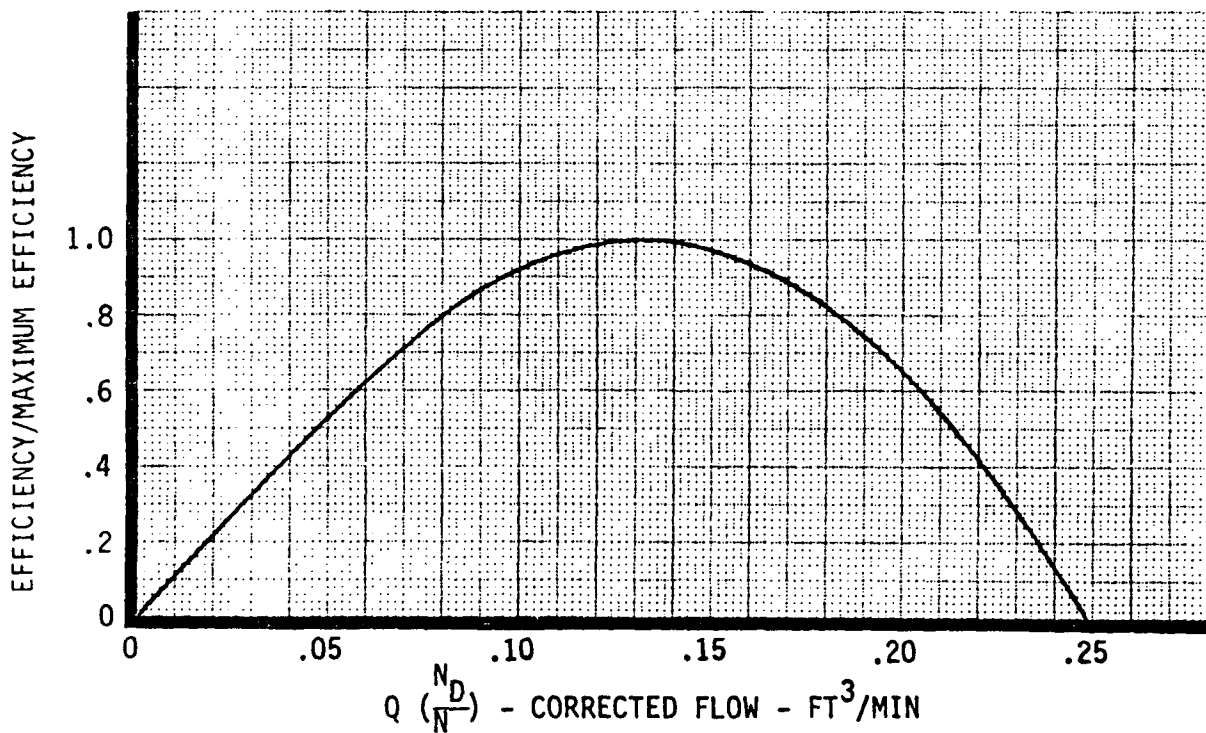ΔT = Difference in wall and fluid temperature

FIGURE 3-2. PUMP HEAD RISE

FIGURE 3-3. PUMP NORMALIZED EFFICIENCY

3.1.2 Loop Model (continued)

R_e = Reynolds Number

P_R = Prandtl Number

μ = Fluid viscosity

μ_w = Fluid viscosity evaluated at wall temperature

The flow rate is variable along the line due to fluid expansion resulting from the heat transfer. The dependence of flow rate on heat transfer requires an iterative solution of the pump pressure rise, line pressure drop, and heat transfer equations. The iteration procedure adjusts the flow from the tank into the loop until the pressure drop matches the pump pressure rise. The iteration procedure is described in detail by Reference 2.

3.1.3 Executive Logic

The program executive provides the necessary interface between the loop and tank models. The structure of the executive was determined by two assumptions concerning basic performance features of the system:

a. The tank pressure responds to the flow and heat input from the loop.

b. The flow from the loop to the tank depends on the pressure change rate in the tank.

The tank and loop are elements of a single thermodynamic system. The above two assumptions are necessary to avoid iteration of the loop and tank relationships to obtain a simultaneous solution. The assumptions are warranted by the small size of the loop in comparison with the tank which permits the tank pressure to be used as the system pressure.

The executive establishes the sequence of the solutions of the loop and tank models. The calculations sequence is set by the time steps required for stability of the loop and tank models. The maximum allowed time step for each of the system elements is used as the overall program time step. System elements requiring a shorter time step than the program time step are treated first. These elements are advanced in time to the program time step by repeatedly solving the element equations for the short time step until the accumulated time is equivalent to the maximum. For example, if the tank time step is 1 second and the loop time step is .1 second, the loop is solved 10 times for each program time step. The flow rates from the loop are accumulated for the several time steps required to provide the necessary flow input to the tank model.

The method used for the loop calculation is based on the pump rpm. When the pump speed is less than 100 rpm, the tank model is used to represent the lines. The pump relationships and steady flow pressure drop equations are used when pump speed is greater than 100 rpm. The executive controls

3.1.3 Executive Logic (continued)

the transfer between the two calculation methods and sets initial conditions and boundary values to conserve mass and energy. A complete description of the executive logic is contained in Reference 2.

3.2 TASK 2 - MODEL VERIFICATION

Test data were not available to verify the ability of the model to accurately simulate external loop pressurization system performance. Model verification was therefore limited to confirming the calculations for basic thermodynamics and fluid flow phenomena.

3.2.1 Tank Stratification Model

The tank model was developed by modification of the stratification model which was verified by comparison with the Apollo oxygen tank performance (References 3 and 4). Only changes made to this program therefore required verification. The major program change was modification of the momentum equation to improve the ability to simulate the jet of fluid injected from the loop.

The modified momentum equation was intended to exactly conserve fluid momentum and kinetic energy in an inviscous fluid. This capability was verified by introducing a disturbance into the tank with the fluid viscosity set to zero and free slip conditions at the boundary. After the initial time step, the total kinetic energy in the tank remained constant with the modified equations but decayed rapidly with the original stratification model.

The ability to simulate a viscous jet flow was verified by comparison with the known solution of a two-dimensional laminar jet. The simulation used a 9-foot square region with fluid injected in a 1-foot wide strip at the top. The same quantity of fluid was withdrawn at the bottom to maintain constant pressure in the box region. The kinetic energy in the container increased smoothly (Figure 3-4) to a steady value when the steady-state flow field (Figure 3-5) was developed. The available jet solution (Reference 5) used for comparison is

$$U = .454 \left(\frac{K^2}{\nu} \right)^{1/3} \frac{1}{\sqrt[3]{Y}} \ (1 - \tanh^2\xi)$$

$$V = .550 \left(\frac{K\nu}{Y^2} \right)^{1/3} [2\xi(1 - \tanh^2\xi) - \tanh\xi]$$

where

U = Velocity parallel to jet centerline
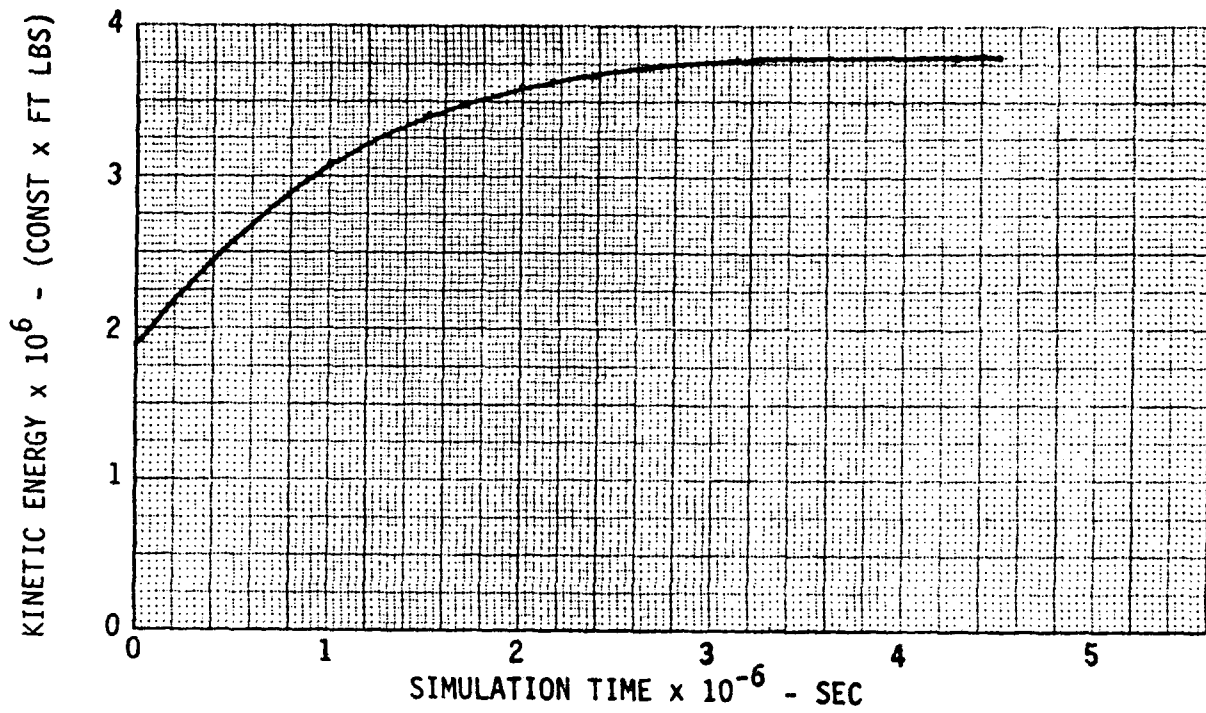
V = Velocity perpendicular to jet centerline
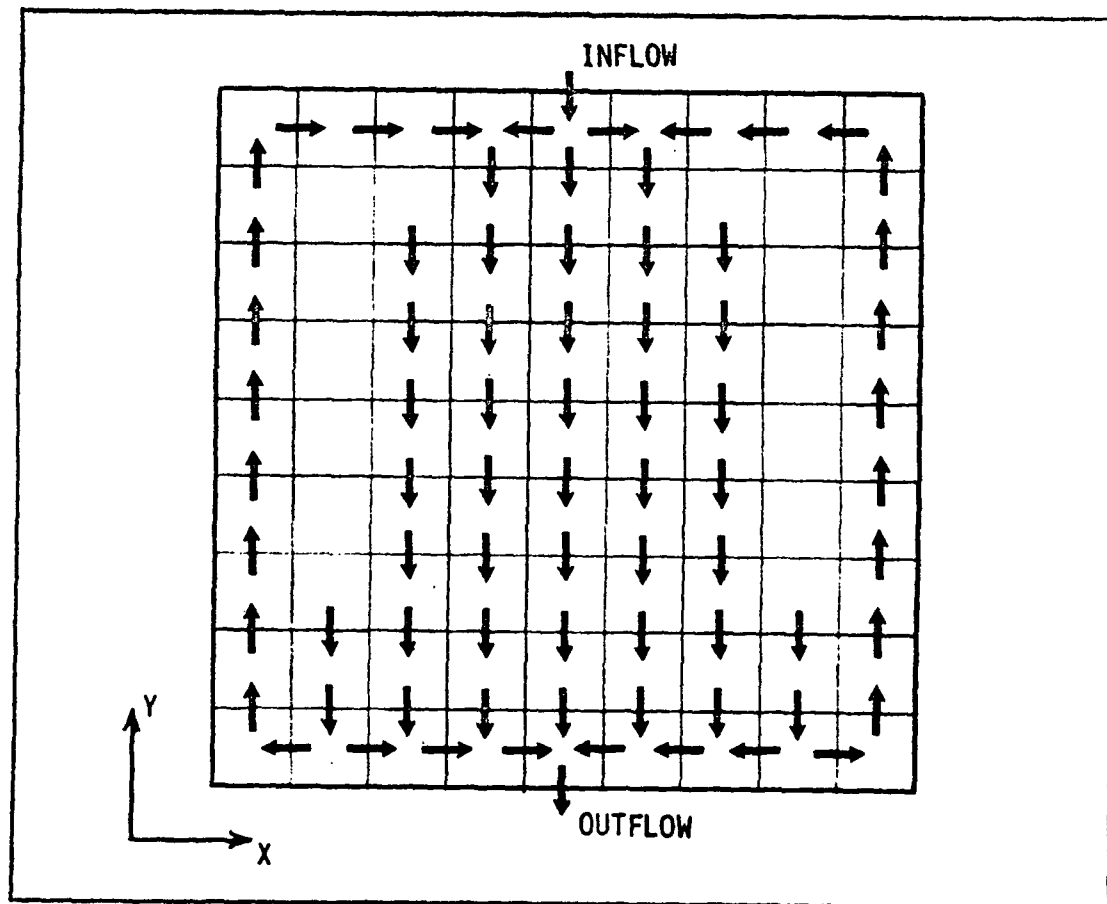
FIGURE 3-4. NET KINETIC ENERGY OF TANK FLUID

FIGURE 3-5. DIRECTION VECTOR PLOT OF JET FLOW FIELD

3.2.1 Tank Stratification Model (continued)

$$\xi = .275 \left(\frac{K}{\nu^2} \right)^{1/3} \frac{X}{Y^{2/3}}$$

K = Kinematic momentum

ν = Kinematic viscosity

X = Perpendicular distance away from jet centerline

Y = Distance from jet orifice on jet centerline

The Reynolds Number of the jet was 9.3 based on the jet width and velocity at the entrance to the box. The finite size of the box caused the jet profiles to deviate from the infinite medium solution. The flow entrained in the downward jet required an equivalent flow upward along the right and left borders (Figures 3-5 and 3-6). The velocity profiles did, however, agree fairly well with the infinite medium solution (Figure 3-7). The velocity distribution along the jet centerline was in good agreement with the infinite medium solution except near the bottom of the box where the boundary had significant effect (Figure 3-8).

The "heater" calculations in the tank model were also revised to include heat obtained from the environment and conduction between heater cells. The heater temperature response to environmental heating was as expected (Figure 3-9) and agreed with independent temperature analyses. The heat conduction between heater cells was verified by initializing each heater cell to a different temperature and simulating the response of each cell. The cell temperatures again behaved as expected (Figure 3-10) and agreed with an independent analysis.

3.2.2 Steady Flow Loop Model

The steady flow loop model uses conventional pressure drop and heat transfer relationships which are well established and require no verification. Independent calculations confirmed that the equations were correct in the computer program, and no comparisons with experimental data were made. The energy equation used for the steady flow condition is the same as used by the tank model which was previously verified. The heater temperature equation used is the same form as that used by the tank model but uses the Sieder-Tate heat transfer relationship in place of conduction to the fluid. The accepted validity of this heat transfer equation therefore establishes the validity of the heater calculation. The pump performance was derived directly from experimental data (Figure 3-2); therefore, verification was not required.

3.3 TASK 3 - PARAMETRIC DATA

External loop design variables which affect the systems transient pressure overshoot and undershoot characteristics were investigated parametrically. The approach used was to determine the maximum pressure overshoot and
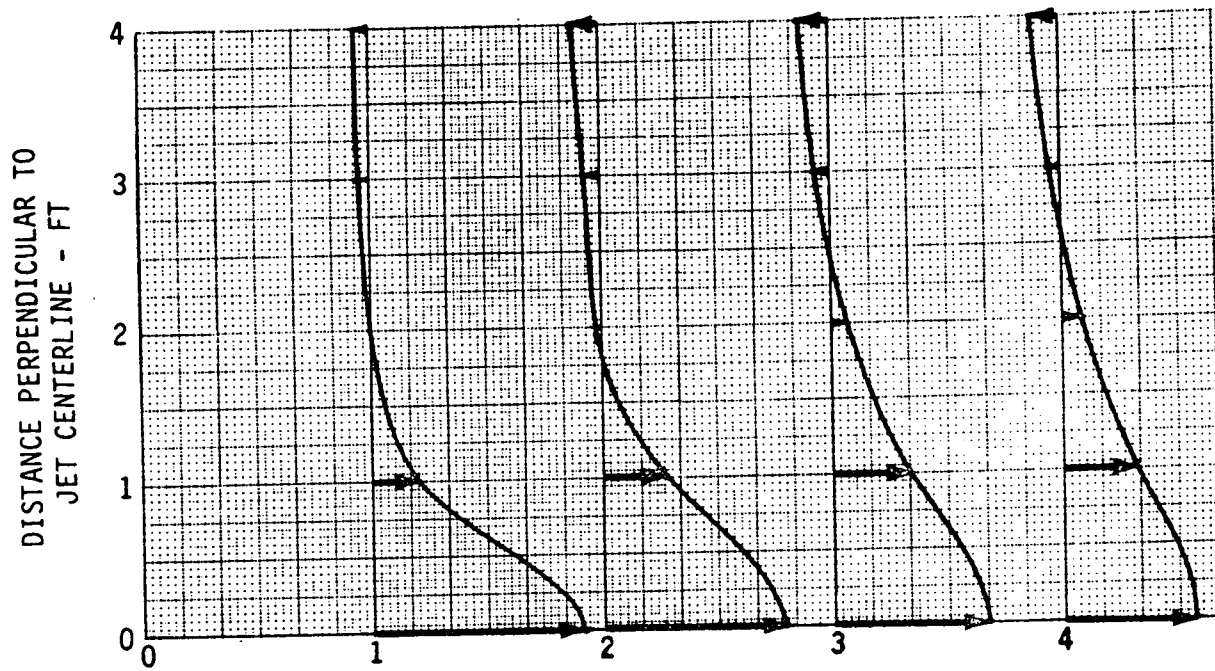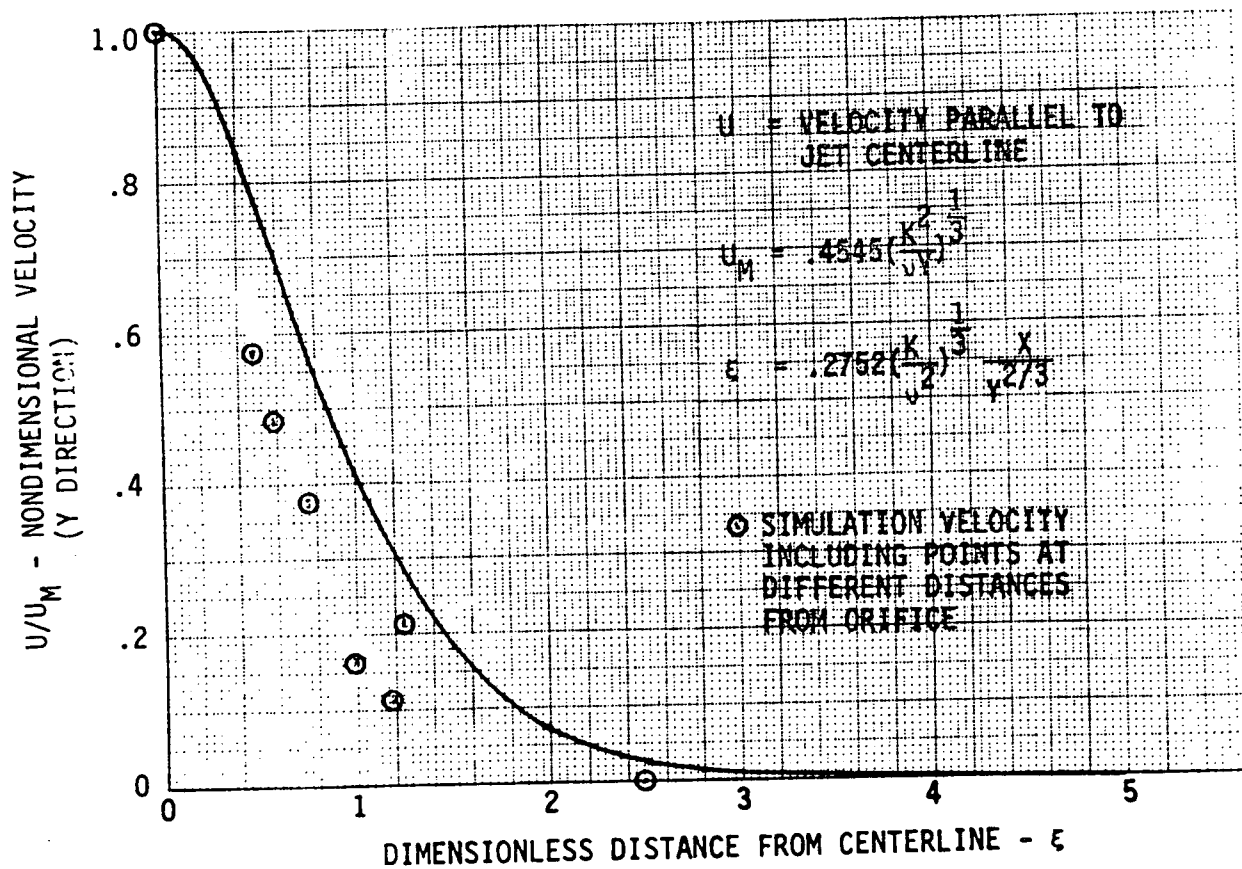
FIGURE 3-6.   VELOCITY PROFILES IN JET FLOW FIELD

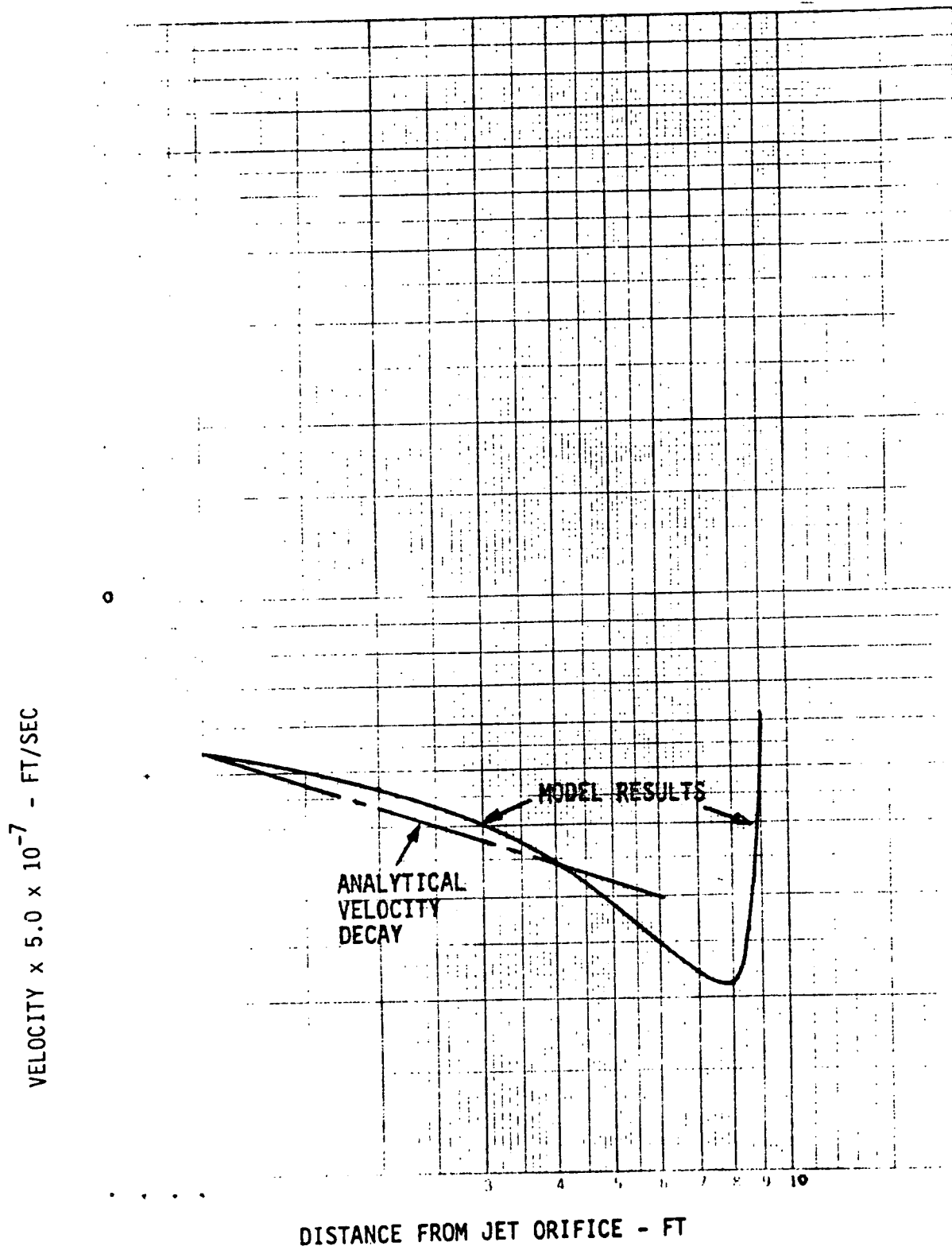FIGURE 3-7.   NONDIMENSIONAL JET VELOCITY PROFILE

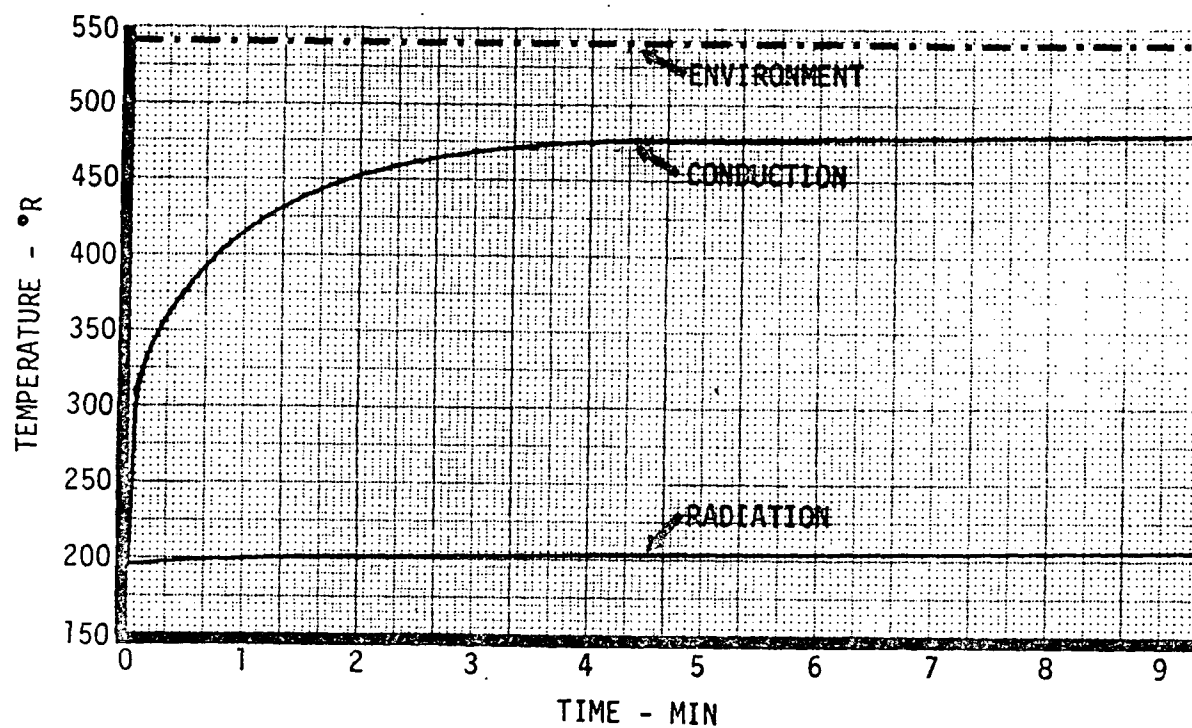FIGURE 3-8. VELOCITY DISTRIBUTION ON JET CENTERLINE

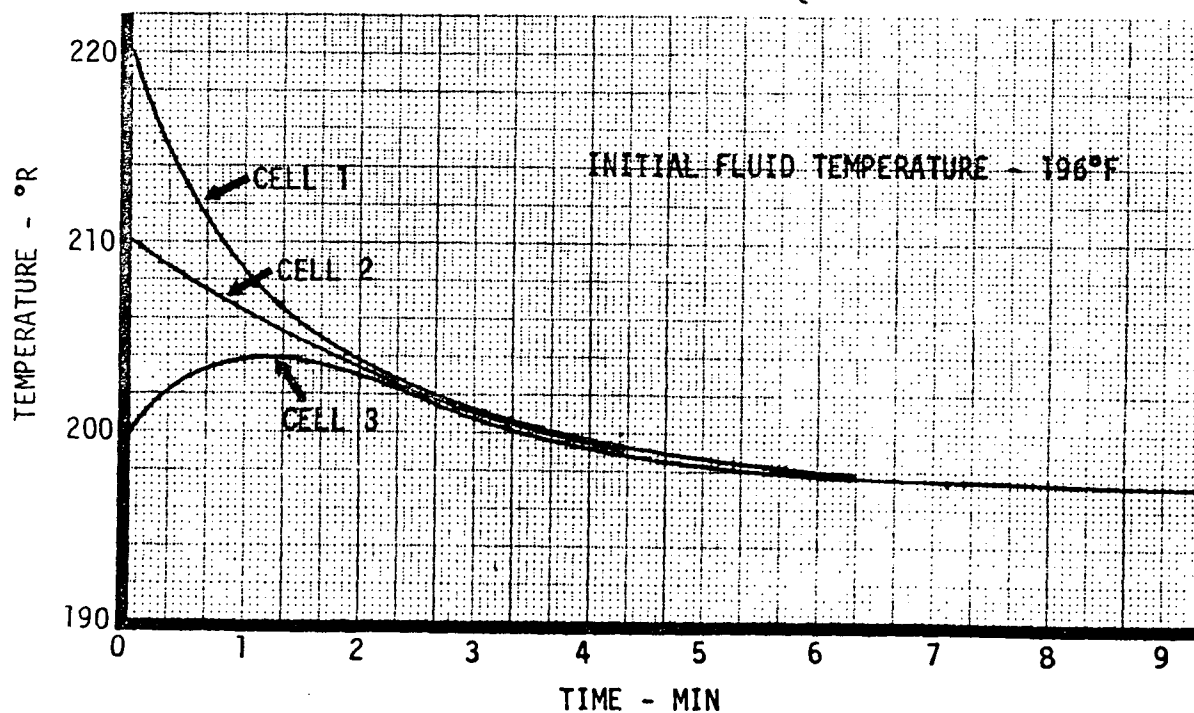FIGURE 3-9. HEATER RESPONSE WITH CONDUCTION AND
RADIATION FROM ENVIRONMENT

FIGURE 3-10. HEATER TEMPERATURE RESPONSE WITH
CONDUCTIVITY BETWEEN CELLS

3.3 TASK 3 - PARAMETRIC DATA (continued)

undershoot which could occur based on worst case conditions. After worst case conditions were established, several design variables were analyzed to determine the effects of each. These detailed analyses were conducted using the computer program (Reference 2) to simulate the tank pressure cycles under typical flight conditions. The basic tank and system data used for the analysis are contained in Appendix A.

3.3.1 System Parameter Effects

General Considerations. Environmental heating of the external loop will cause the fluid in the loop to be at higher temperature and lower density than the tank fluid. The pressure in a supercritical fluid depends on the temperature distribution in the fluid. The system pressure is a minimum with a uniform temperature throughout the fluid. When the fluid is heated locally, the pressure rises above the equilibrium (uniform temperature) pressure. The difference between the actual pressure and the equilibrium pressure is conveniently referred to as the "potential pressure decay." The potential pressure decay is the pressure undershoot which will occur if the fluid is mixed to obtain equilibrium conditions. If the potential pressure decay develops from an initially equilibrium condition, a pressure increase or overshoot will occur. The effects of the low-density fluid in the loop volume were evaluated using simplified methods to provide a basis for subsequent analysis.

Potential pressure changes resulting from the different density fluid in the loop and tank were evaluated using the methods developed in Appendix B. These data (Figures 3-11 and 3-12) provide a method for estimating the pressure changes which result from the loop heating. The pressure change is proportional to the ratio of the line volume to the tank volume. Pressure excursions can therefore be controlled by limiting the loop volume. For example, if the loop-to-tank volume ratio is 1/1000, the maximum pressure decay for 70 lbs/ft^3 oxygen is approximately 56 psi. Reducing the loop volume by a factor of two will reduce the pressure decay to 28 psi. Pressure decays in hydrogen are less severe than in oxygen. A loop-to-tank volume ratio of 1/1000 produces a maximum pressure change of approximately 9 psi for hydrogen.

The potential pressure change is strongly affected by the density of the loop fluid (Figures 3-11 and 3-12). The loop will be filled with high-density fluid while the pump is on, but the density will decrease while the pump is off due to environmental heating. The density change as a function of time can be estimated from the fluid expulsion energy requirements (Figure 3-13) if the heating rate is known. Since the expulsion energy requirement is greater for oxygen than for hydrogen, the oxygen potential decay will increase at a slower rate but will reach a higher maximum value.

Injection Velocity Effects. The related effects of tank acceleration and fluid injection velocity were explored for high-density (69.48 lbs/ft^3) oxygen. One complete pressure cycle was simulated at 10^{-7} "g" acceleration and an injection velocity of approximately .01 ft/sec. The potential pressure
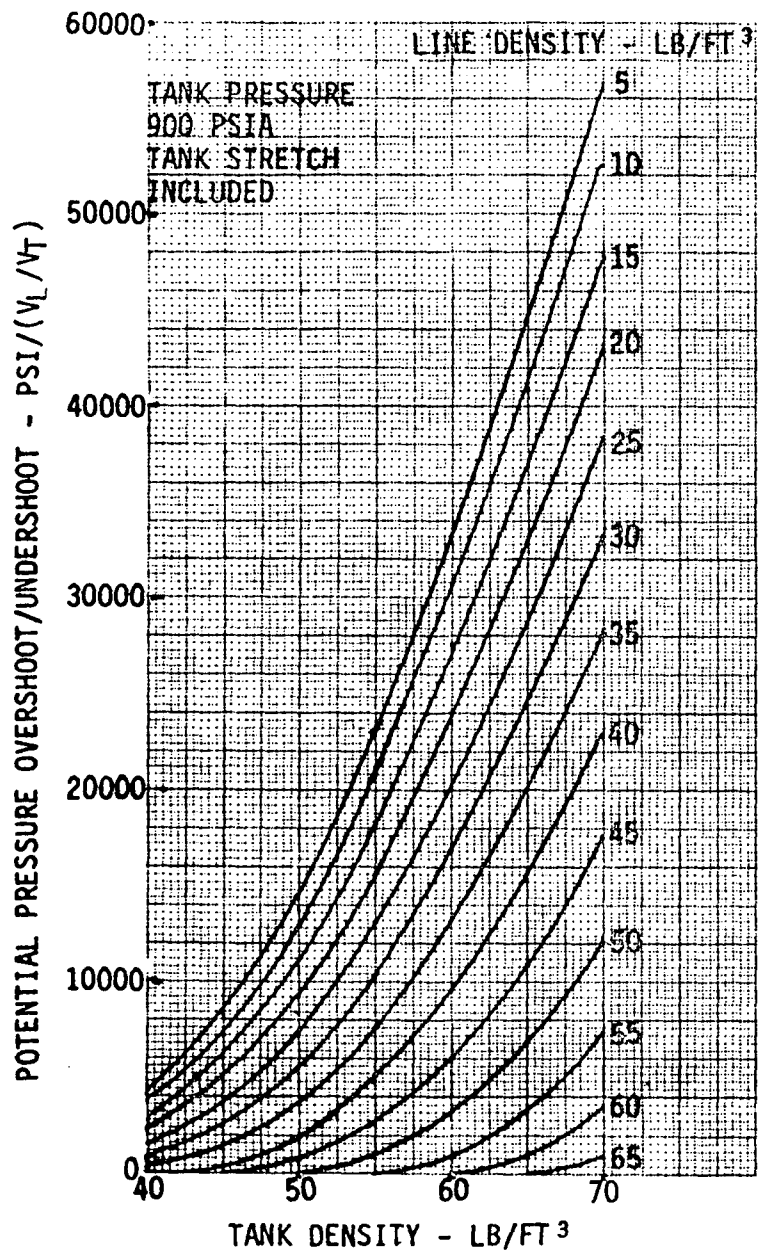
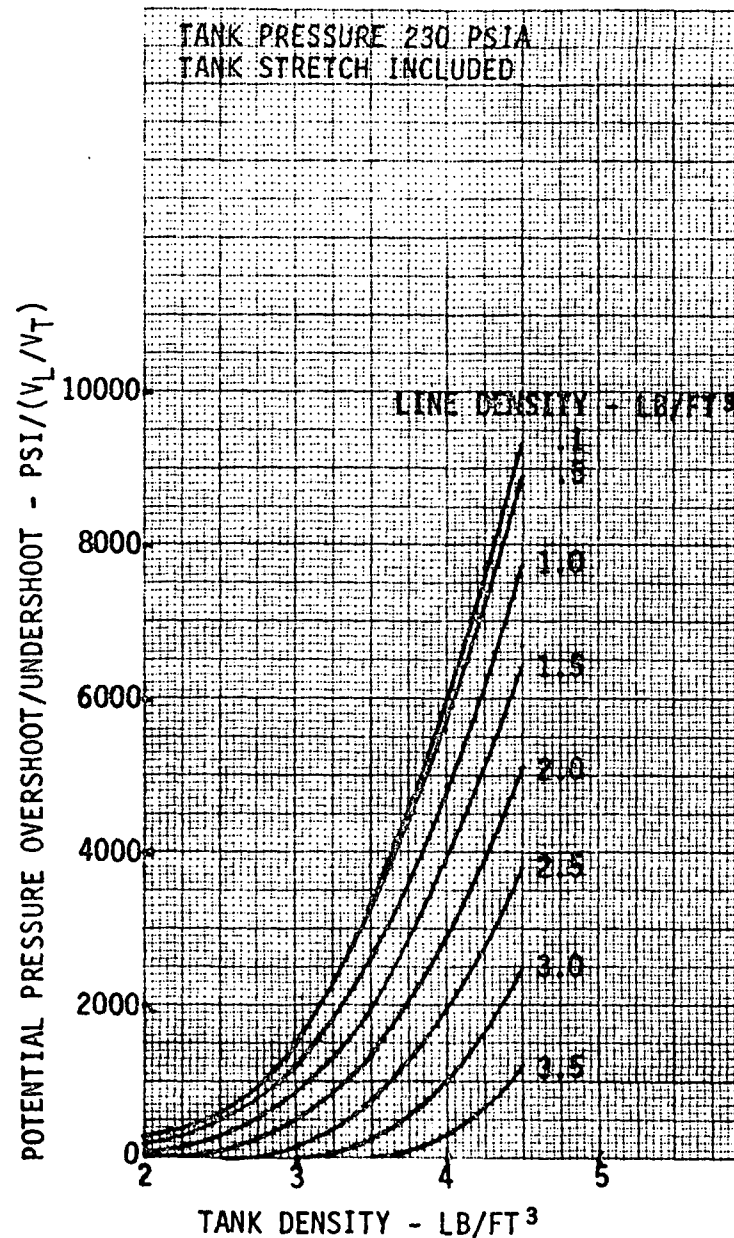FIGURE 3-11. OXYGEN TANK PRESSURE
OVERSHOOT/UNDERSHOOT

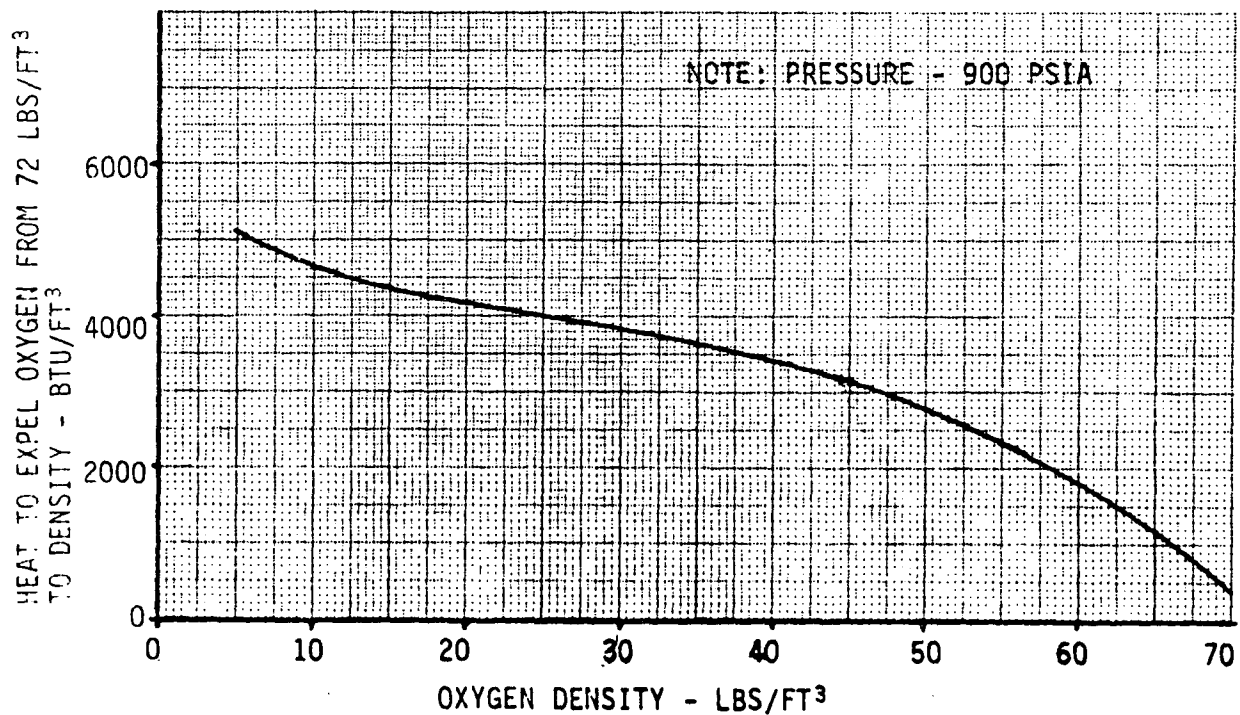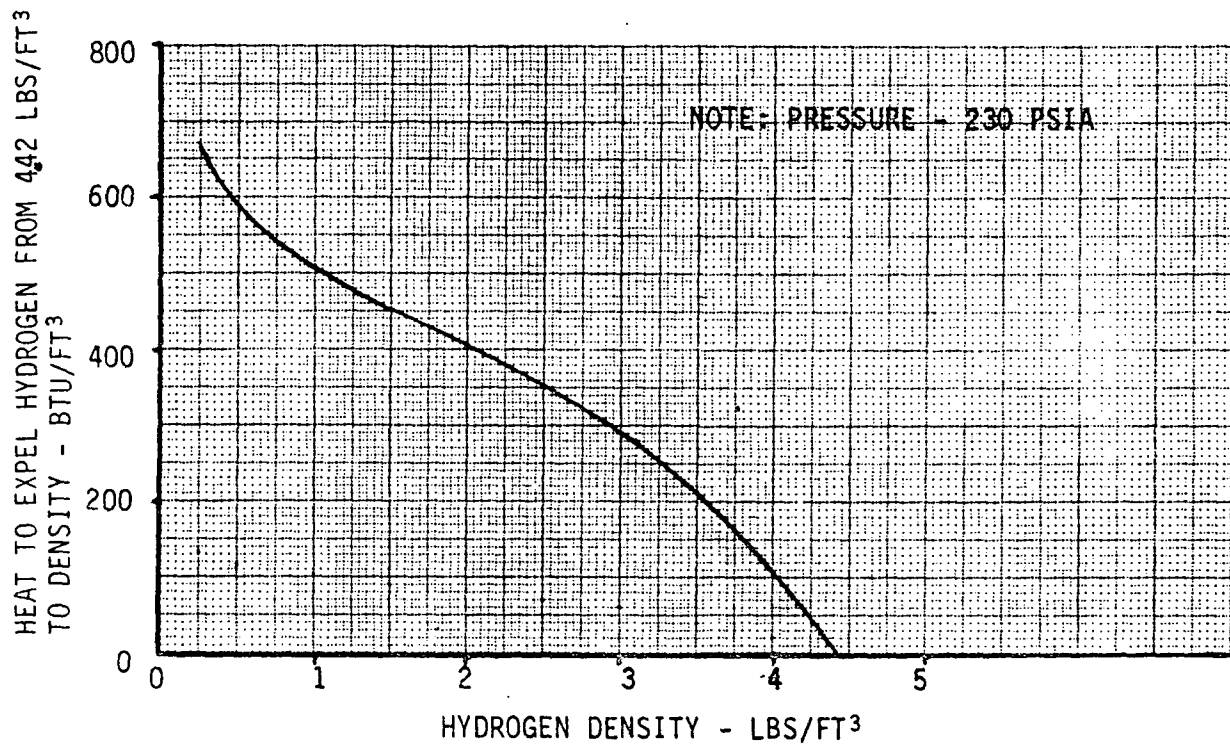FIGURE 3-12. HYDROGEN TANK PRESSURE
OVERSHOOT/UNDERSHOOT

FIGURE 3-13.   FLUID EXPULSION ENERGY REQUIREMENTS

3.3.1 System Parameter Effects (continued)

decay computed for the fluid in the tank only was less than 1.6 psi throughout the pressure cycle. The simulation was repeated with a finer grid and with the injection velocity increased by a factor of two. The tank potential pressure decay was reduced to .86 psi by the higher injection velocity confirming that the low value of the potential pressure decay was a result of mixing and not the grid size. Injection velocities will certainly be greater than the .01 ft/sec investigated, and the acceleration will probably be greater than 10^{-7} "g". These "worst case" conditions produced negligible stratification and potential pressure decay in the tank; therefore, injection velocity and acceleration were not further investigated. These results confirmed that the tank could be adequately treated using a coarse grid for the model. The effect of injection velocity in the hydrogen tank was not investigated since hydrogen potential pressure decay is generally less than the oxygen decay.

Loop Volume Effects. The effect of loop volume on the system potential pressure decay was investigated with the complete math model to determine if the simplified analysis (Figures 3-11, 3-12, and Appendix B) provided good results. Two high-density oxygen conditions were simulated with loop-to-tank volume ratios of .0004 and .0002 (Figure 3-14). The maximum potential pressure decays resulting from the two simulations were within .4 psi of the decay obtained from the simplified method. This agreement confirms that the potential pressure decay can be scaled with the ratio of the loop-to-tank volume. It was concluded from this result that the remainder of the analyses could be conducted using the same loop and tank volumes.

Loop Heat Leak Effects. The external loop is filled with cold fluid during the pump on (pressurization upstroke) period. Loop heating effects are therefore most significant when the pump is off during the downstroke. Rapid heating of the fluid in the loop can cause the pressure to rise after the pump and heater are turned off at the upper pressure switch setting.

Two hydrogen downstrokes were simulated with different heat inputs to the loop. The heating of the lines was assumed to be due to radiation heat transfer only. The simulations were conducted with the lines radiation absorptance (α) of .2 and .1. The radiation area for each of the two lines was taken as .7293 ft^2 and the thermal mass of each line was .01 Btu/°R. These radiation heating parameters caused the pressure to overshoot the pressure switch setting (240 psia) for the high-density low-flow condition simulated (Figure 3-15). The pressure overshoot is closely related to the potential pressure decay and the flow from the loop to the tank. The peak pressure occurs later than the maximum of the flow from the loop. Each of the heating rates (α = .1 and .2) raised the line fluid temperature to near ambient (530°R) and produced the same maximum potential pressure decay. The system pressures were significantly different during the initial part of the downstroke. The pressures converged to the same value when the fluid in the lines approached ambient temperature.

Oxygen downstrokes were simulated with line radiation absorptances of .2, .4, and .6. The line radiation areas were the same as for the hydrogen

OXYGEN DENSITY = 69.48 LBS/FT^3
LINE THERMAL MASS = .1 BTU/°F
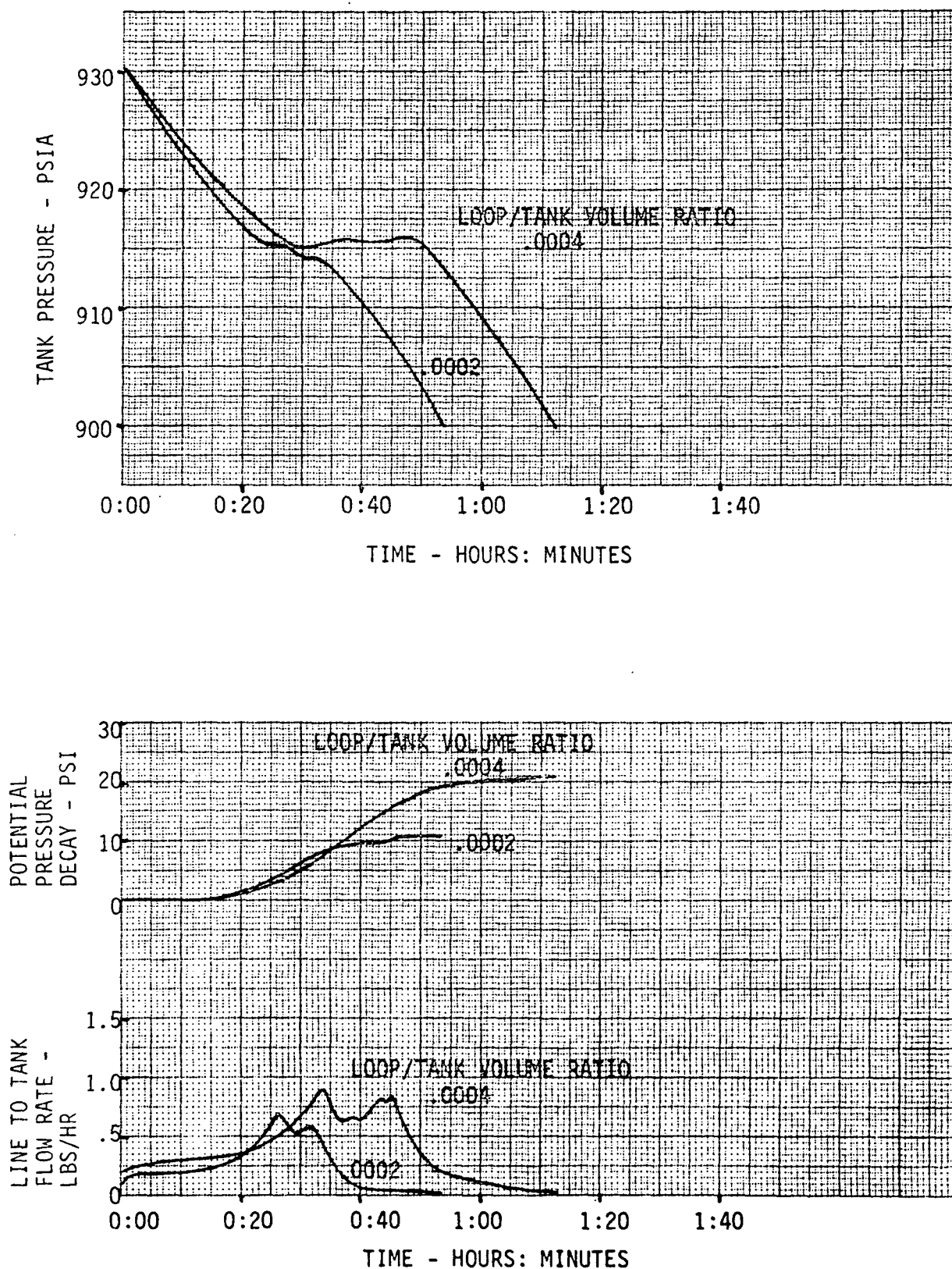DEMAND FLOW = 1.25 LBS/HR
RADIATION ABSORPTANCE .4

FIGURE 3-14. EFFECT OF LINE HEATING ON OXYGEN
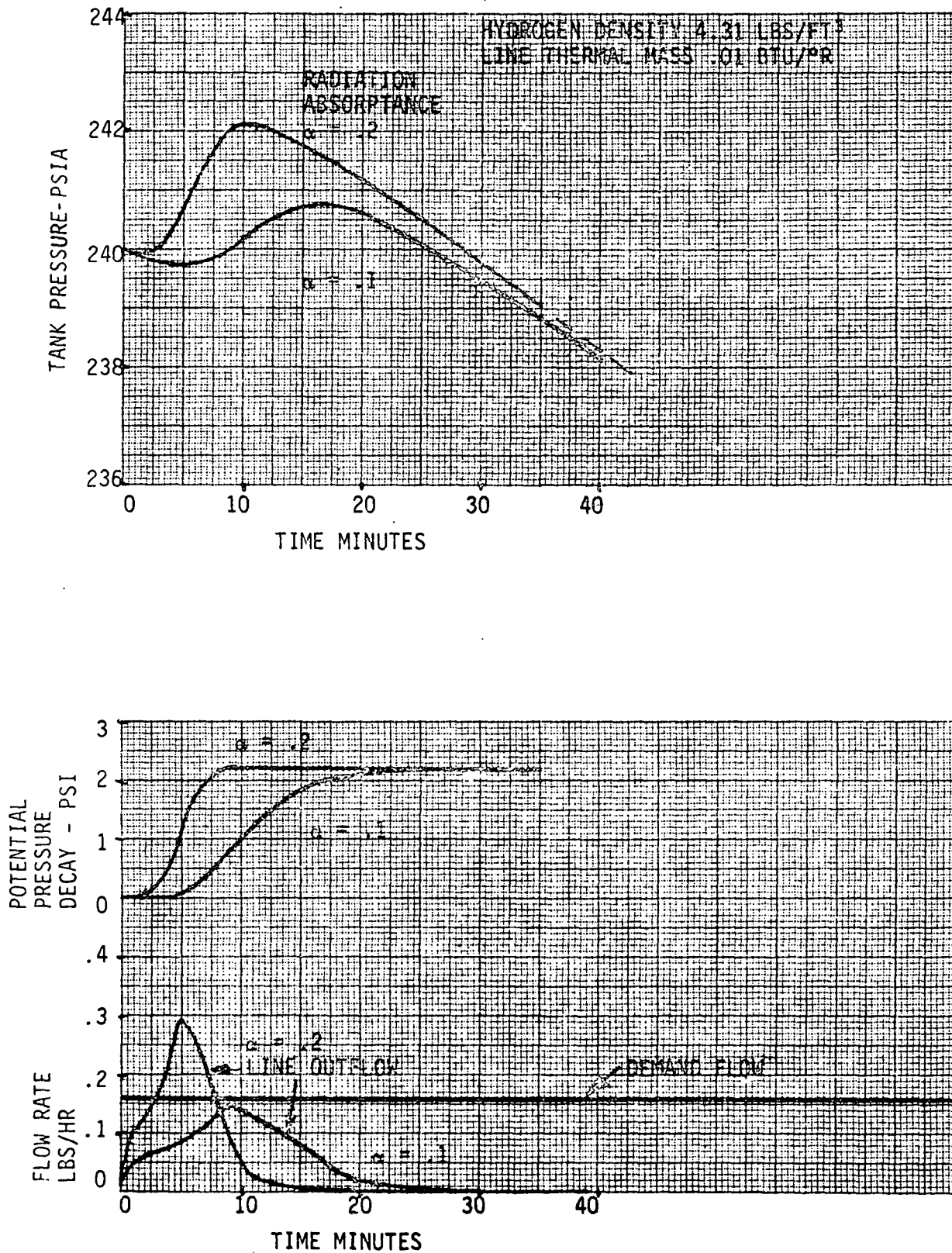OVERSHOOT AT 100% TANK QUANTITY

FIGURE 3-15.   EFFECT OF LINE HEATING ON HYDROGEN OVERSHOOT

3.3.1 System Parameter Effects (continued)

simulations (.7293 ft^2), but the thermal mass of each line was taken as .1 Btu/°R. The oxygen pressure did not increase above the pressure switch setting (930 psia) for the heating rates investigated (Figure 3-16). The maximum heating rate (α = .6) did cause a peak in the pressure time trace, but the maximum value did not exceed the pressure switch limit. The low heating rate (α = .2) pressure trace differed only slightly from that expected for equilibrium conditions. The potential pressure decay at the bottom of the downstroke (900 psia) was nearly the same for the two higher heating rates (20 to 22 psi). The lower heating rate, however, produced less than 2 psi potential pressure decay because the line fluid density remained above the critical region, and flow rates from the line to the tank were small.

Loop Thermal Mass Effects. The thermal mass of the loop strongly affects the pressurization upstroke because the stored heat energy is rapidly added to the fluid when the pump is turned on. Hydrogen pressurization strokes were investigated with the thermal mass of each line taken as .01, .03, and .05 for successive simulations. The initial line temperature was 509°R to represent worst case conditions. The pressure increase resulting from cooling the lines was approximately 16 psi with the .05 Btu/°R thermal mass (Figure 3-17). The time required for the pressure increase is less than that shown by the simulation results. It was necessary to limit the fluid heating rate in the model to obtain stability; therefore, the simulated pressure rise is less rapid than expected. The overall pressure increase is accurate however. The overall pressure increase can be determined from

$$\Delta P = C \frac{\phi}{V} MCp (Ta - Tf)$$

where

ΔP = Pressure increase

C = Tank stretch factor

$$\phi = \frac{1}{\rho \frac{\partial u}{\partial P}}$$

ρ = Fluid density

u = Fluid internal energy

P = Pressure

MCp = Thermal mass

Ta = Ambient or line initial temperature

Tf = Fluid or line final temperature

This equation is in nearly exact agreement with the simulation results and may be used to determine the maximum allowable thermal mass. The tolerable pressure increase is, at most, the difference between the relief pressure
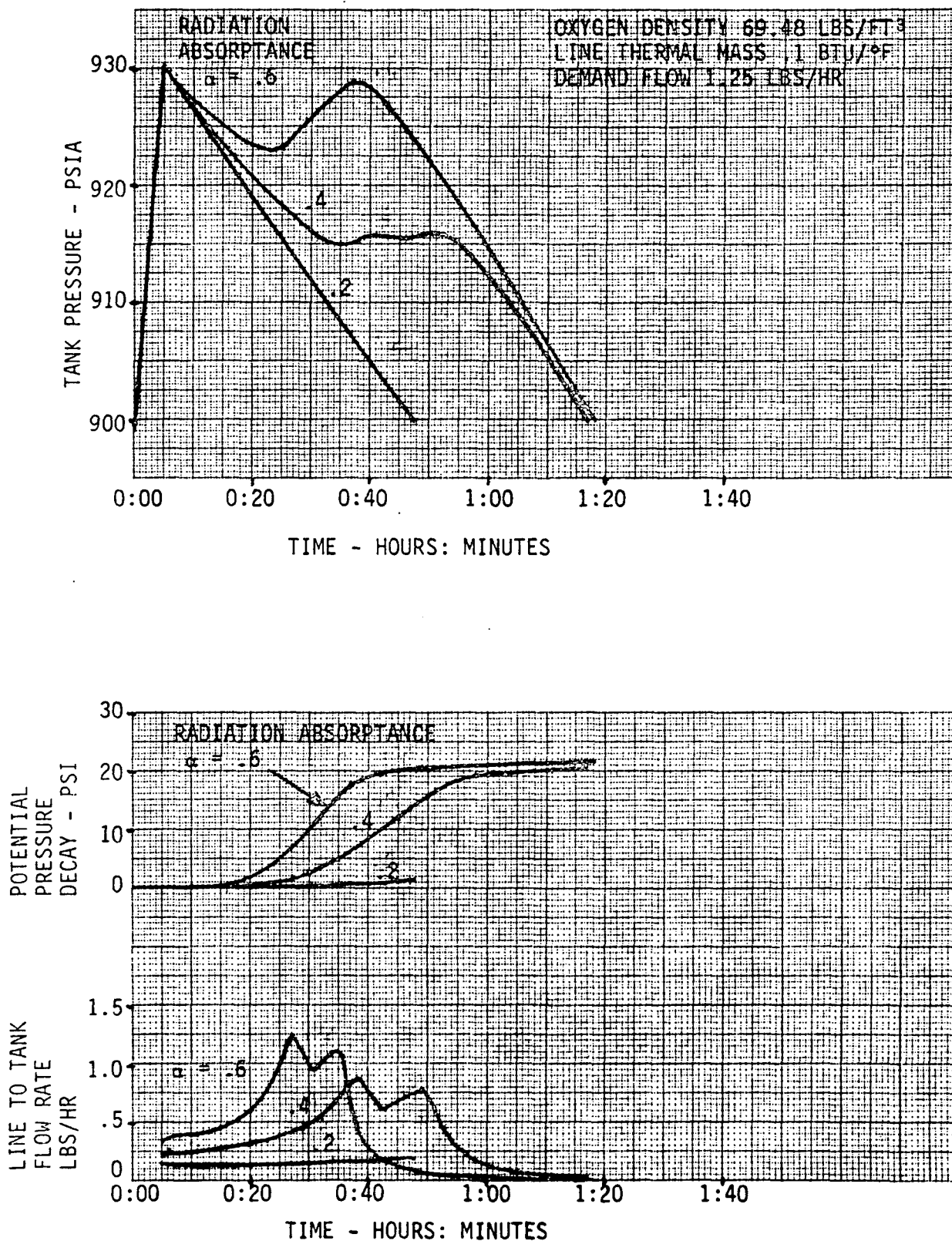
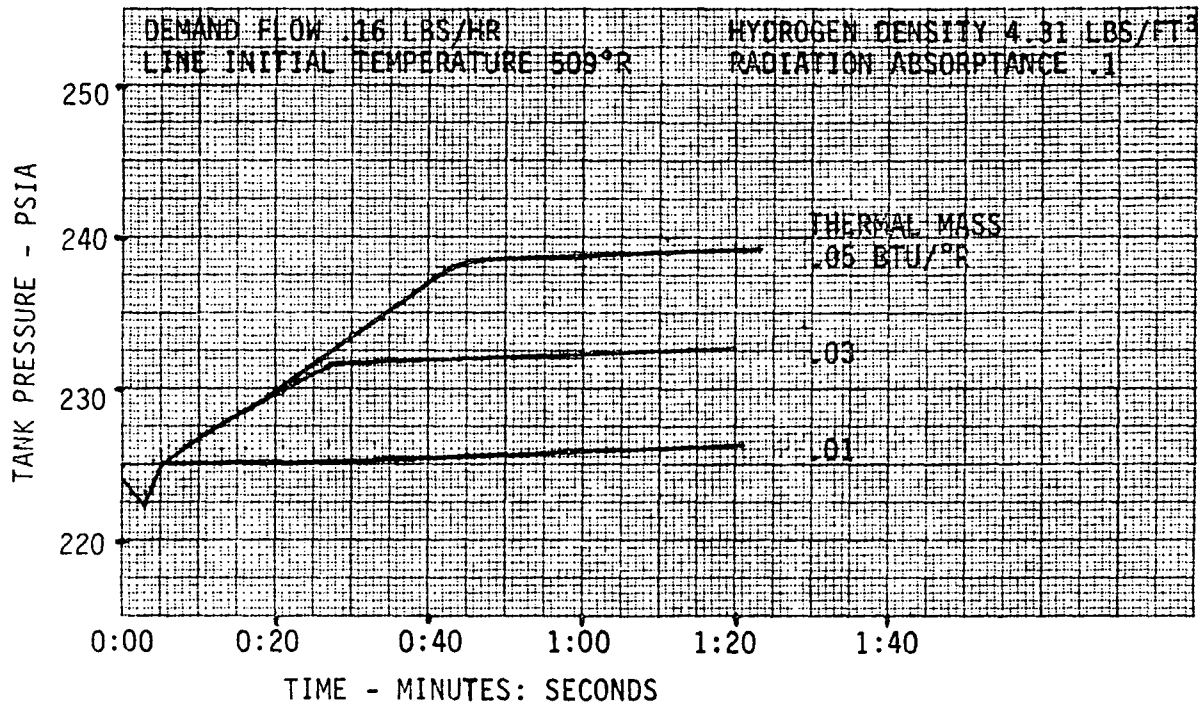FIGURE 3-16. EFFECT OF LINE HEATING ON OXYGEN OVERSHOOT

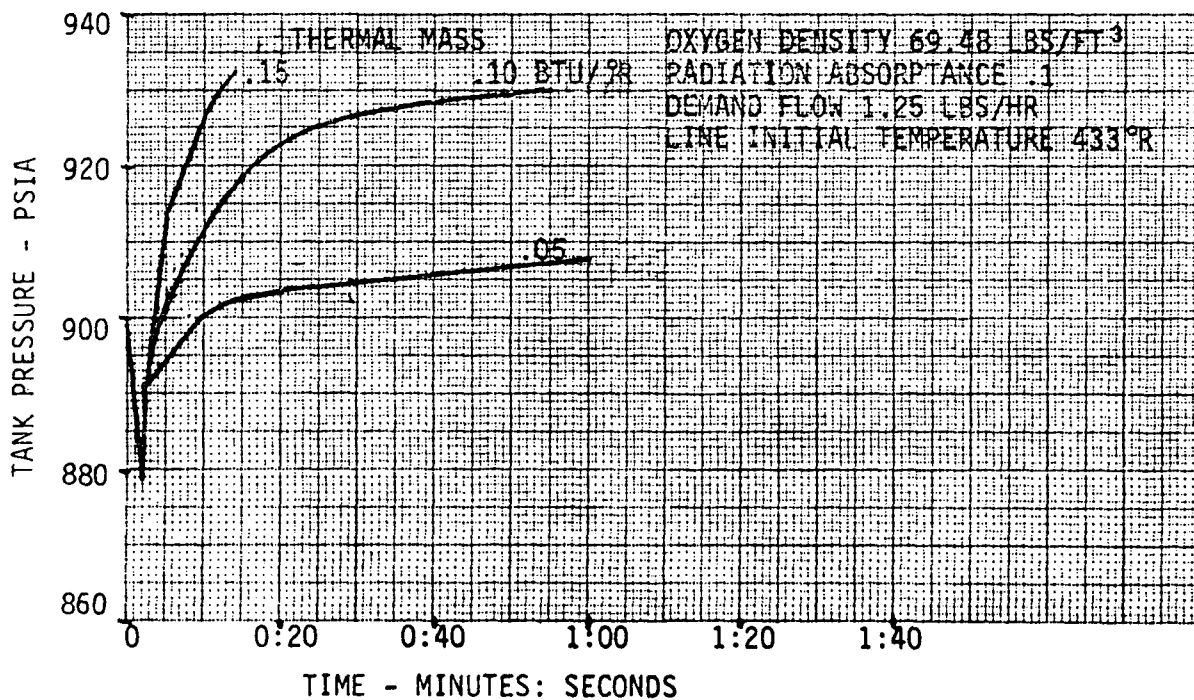FIGURE 3-17. EFFECT OF LINE THERMAL MASS
ON HYDROGEN PRESSURIZATION

FIGURE 3-18. EFFECT OF LINE THERMAL MASS
ON OXYGEN PRESSURIZATION

3.3.1 System Parameter Effects (continued)

and the lower pressure switch setting. Using this pressure difference and solving the previous equation for thermal mass provides the maximum allowable thermal mass. Based on this relationship, the allowable thermal mass is directly proportional to the tank volume.

The oxygen pressurization strokes also exhibited a rapid pressure increase due to the heat stored in the loop thermal mass (Figure 3-18). The thermal mass of .15 Btu/°R for each line caused the pressure to rise from 880 psia to 930 psia (the upper pressure limit) before the line was completely cooled down. These results indicate that the thermal mass of each of the lines should be less than .1 Btu/°R for an 18-ft^3 tank to maintain pressure below the upper pressure switch limit. The oxygen pressure rises were approximately in agreement with the simplified analysis used for hydrogen. The simulated pressure rise was, however, greater than indicated by the simplified method, and the cause of the discrepancy was not positively identified. The heat content of the fluid in the loop contributed part of the error, but including this factor did not provide complete agreement.

The loop thermal mass also affects the pressure downstroke and the overshoot characteristics. Increasing the thermal mass reduces the overshoot caused by line heating. Increasing the thermal mass of the hydrogen loop from .01 to .05 Btu/°R/line delayed the peak in the pressure trace (Figure 3-19) and prevented the pressure from exceeding the pressure switch limit. The delay and depression of the pressure peak are caused by the higher thermal mass of the line absorbing a larger fraction of the heat input from the environment. Two oxygen simulations with a loop thermal mass of .05 and .1 Btu/°R/line also indicated that increasing thermal mass reduced the pressure peak (Figure 3-20).

Pump Spinup Effects. The oxygen tank pressure response was simulated with two pump acceleration rates. The pump and heater were turned on at 899 psia and the pump accelerated to design speed. The lines were initially filled with tank density fluid (69.48 lbs/ft^3). A pump acceleration time of 10 seconds caused the pressure to lag the pressure obtained with a 1-second acceleration time (Figure 3-21). A pressure decrease of .2 psi also occurred with the 10-second acceleration time. The slower acceleration time reduced the heat input from the pump to the fluid since the pump power was lower during the acceleration. The reduced heat input produced about .15 psi pressure difference after both simulations reached steady-state conditions. The slower acceleration also produced a heater temperature overshoot of 13°R (Figure 3-21). The small pressure and temperature differences resulting from the 1 and 10-second pump acceleration times are not significant to the overall system performance.

The heater and pump will probably be turned off simultaneously when the pressure reaches the upper pressure switch limit. This control method prevented any heater temperature overshoot during spindown, and no significant effects were noted with a pump spindown time of one-half second. This result indicates no constraint on pump spindown time is required. Heater temperature overshoot at the beginning of the pressurization stroke will be adequately controlled with acceleration times of less than 10 seconds.
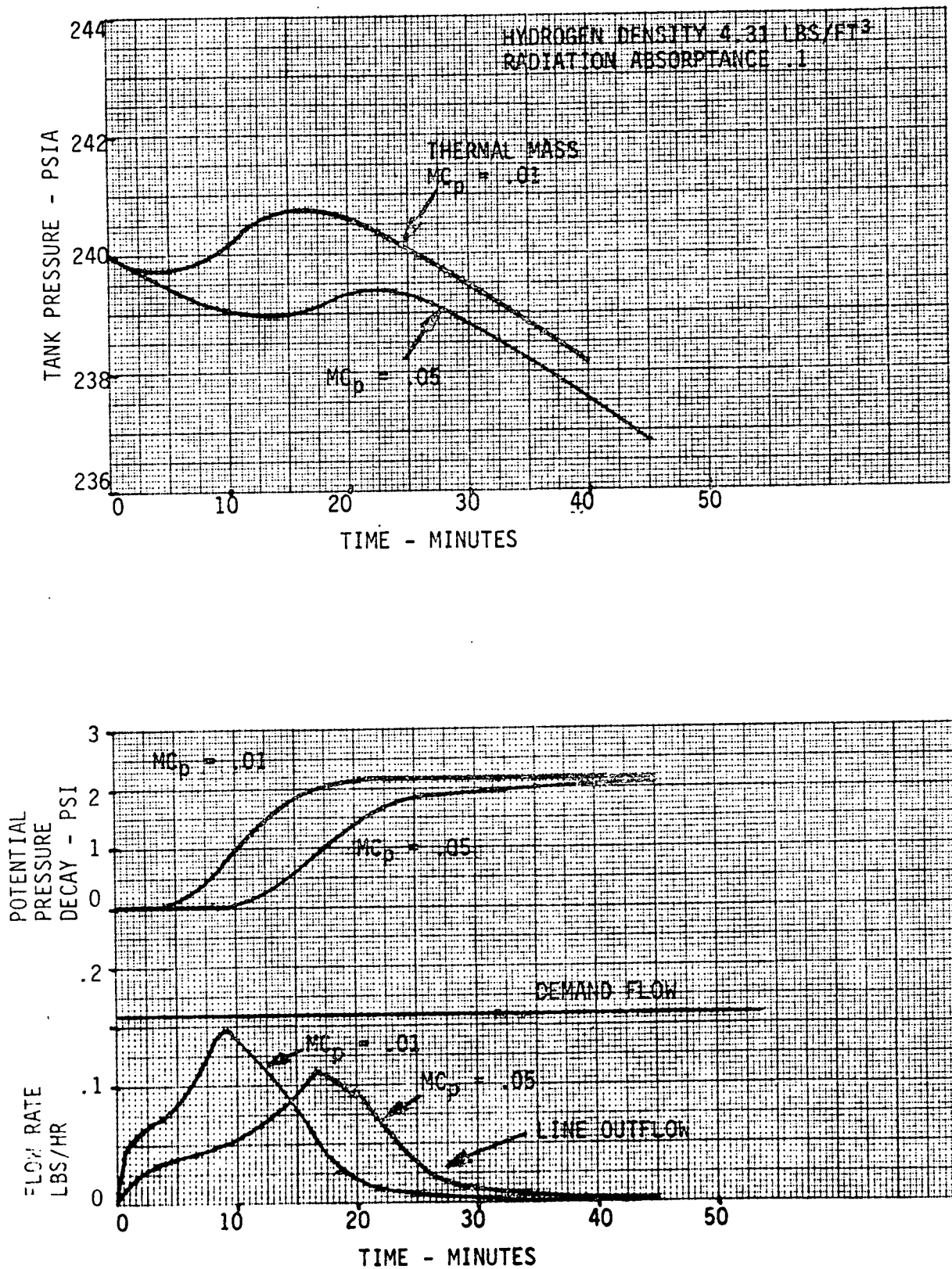
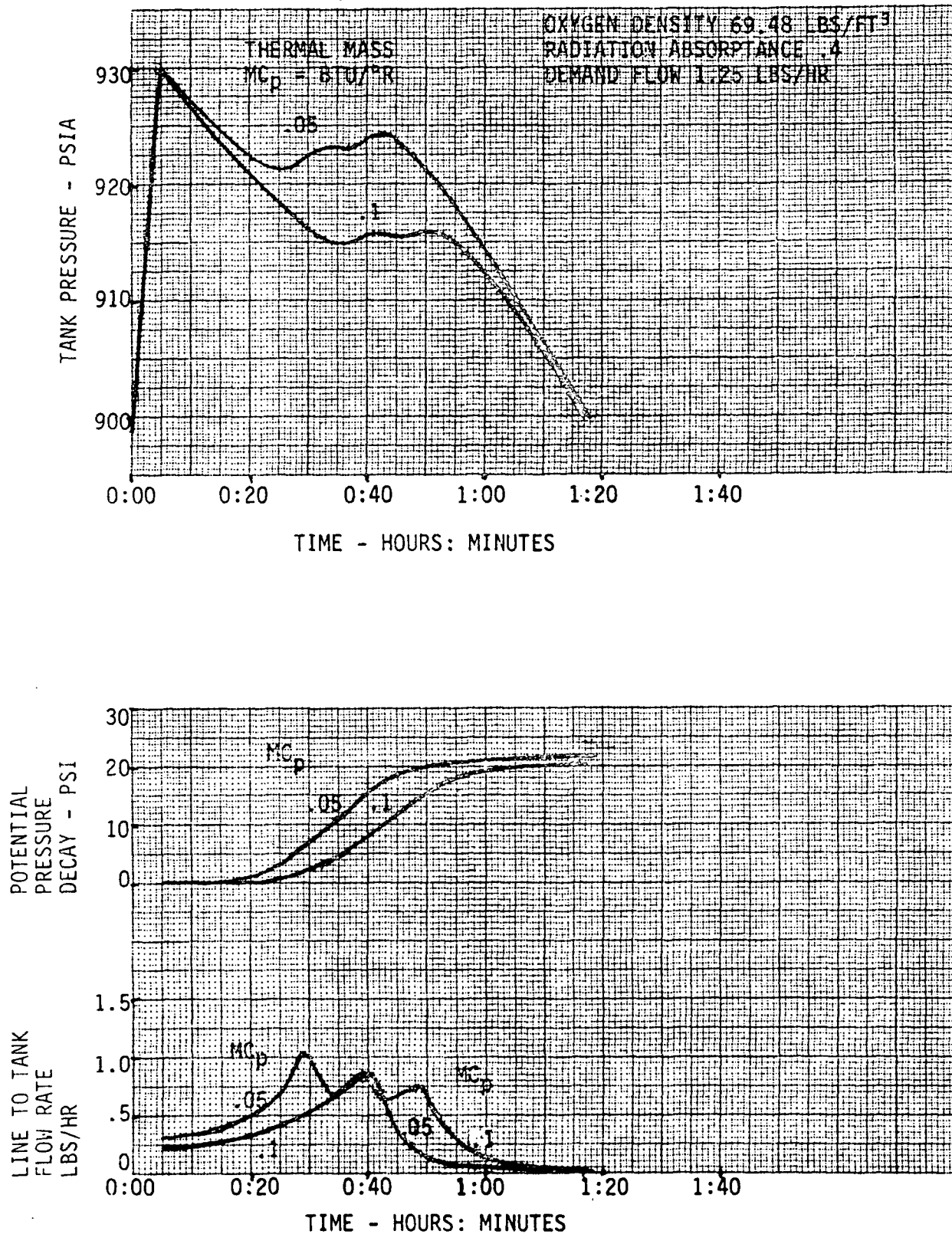FIGURE 3-19. EFFECT OF LINE THERMAL MASS
ON HYDROGEN OVERSHOOT

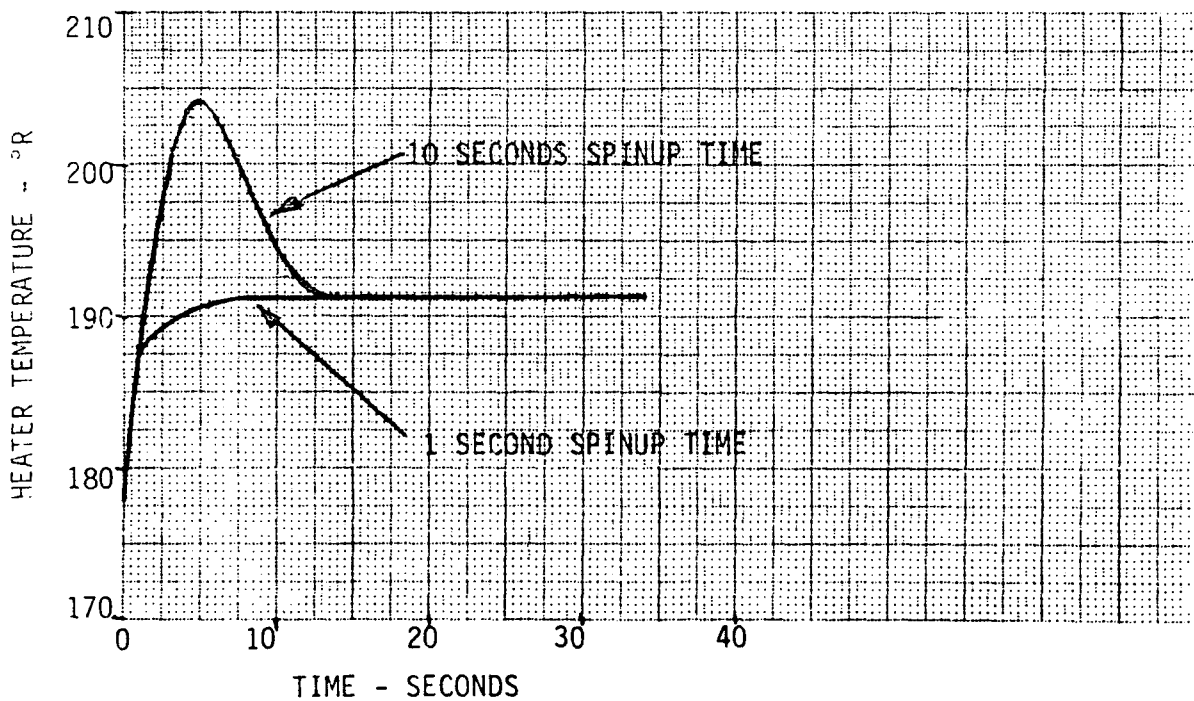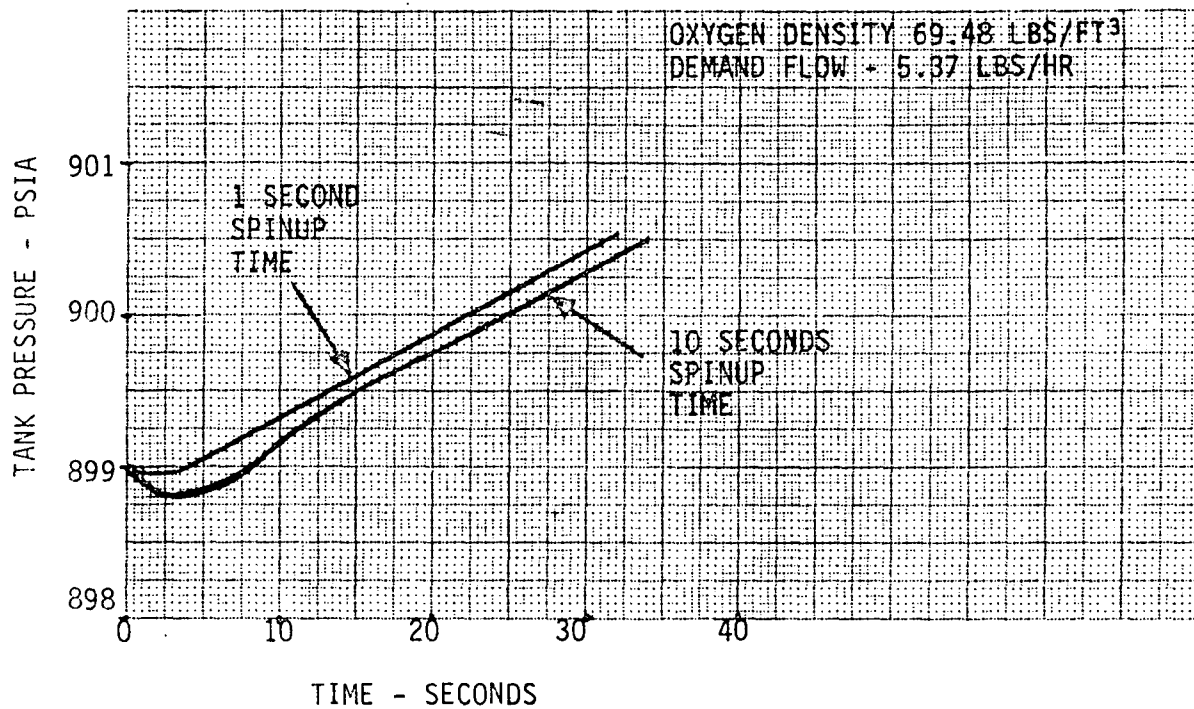FIGURE 3-20. EFFECT OF LINE THERMAL MASS
ON OXYGEN OVERSHOOT

FIGURE 3-21. EFFECT OF PUMP SPINUP RATE
ON OXYGEN PRESSURIZATION

3.3.2 Typical System Performance

Simulations of complete pressure cycles at four different fluid densities were conducted for both hydrogen and oxygen at expected nominal operating conditions (Figures 3-22 through 3-29). The densities were selected to approximately represent 25, 50, 75, and 100% full quantities. The nominal flow rates were 2.7 lbs/hr for oxygen and .32 lbs/hr for hydrogen. The radiation absorptance of the lines was .4 for oxygen and .1 for hydrogen. The thermal mass of the lines was .1 Btu/°R/line for oxygen and .01 Btu/°R/line for hydrogen. The tank heat leak during these simulations was less than expected (44 Btu/hr for oxygen and 15 Btu/hr for hydrogen). The heat leak discrepancy affected the duration of the pressurization stroke but did not significantly affect the transient characteristics.

The heat leak error was caused by the method used to initialize the tank wall temperature. To avoid iteration, the wall temperature is initialized to provide the actual heat leak using thermal conductivity based on the fluid temperature. During the simulation, the heat input to the fluid is based on the conductivity at the average of the wall and fluid temperature. The difference in the two methods of determining thermal conductivity causes the heat input to vary during the simulation until the tank wall temperature adjusts to the correct value. The actual tank heat leak performance is not known at this time, and the simulated values were within the expected heat leak performance range.

No severe pressure excursions outside the control band occurred during the hydrogen or oxygen simulations at the nominal flow conditions. The maximum potential pressure decay (6 psi) for oxygen occurred at the 75% quantity for the 2.7 lbs/hr flow rate. The short duration of the oxygen pressure cycle at the 100% quantity condition caused the loop fluid density to remain near the tank density and resulted in negligible potential pressure decay. The potential pressure decay was also negligible for the oxygen 50% and 25% quantities. The hydrogen simulation at 100% quantity and .32 lbs/hr flow produced 2 psi potential pressure decay which is nearly the same as obtained at .16 lbs/hr flow rate. Less than .5 psi pressure decay occurred during the lower quantity hydrogen simulations.

3.3.3 Combined Potential Pressure Decay Results

Oxygen simulations conducted at a loop-to-tank volume ratio of .0004 and worst case conditions of density (69.48 lbs/ft^3) and flow rate (1.25 lbs/hr) resulted in potential pressure decays shown by the table below.

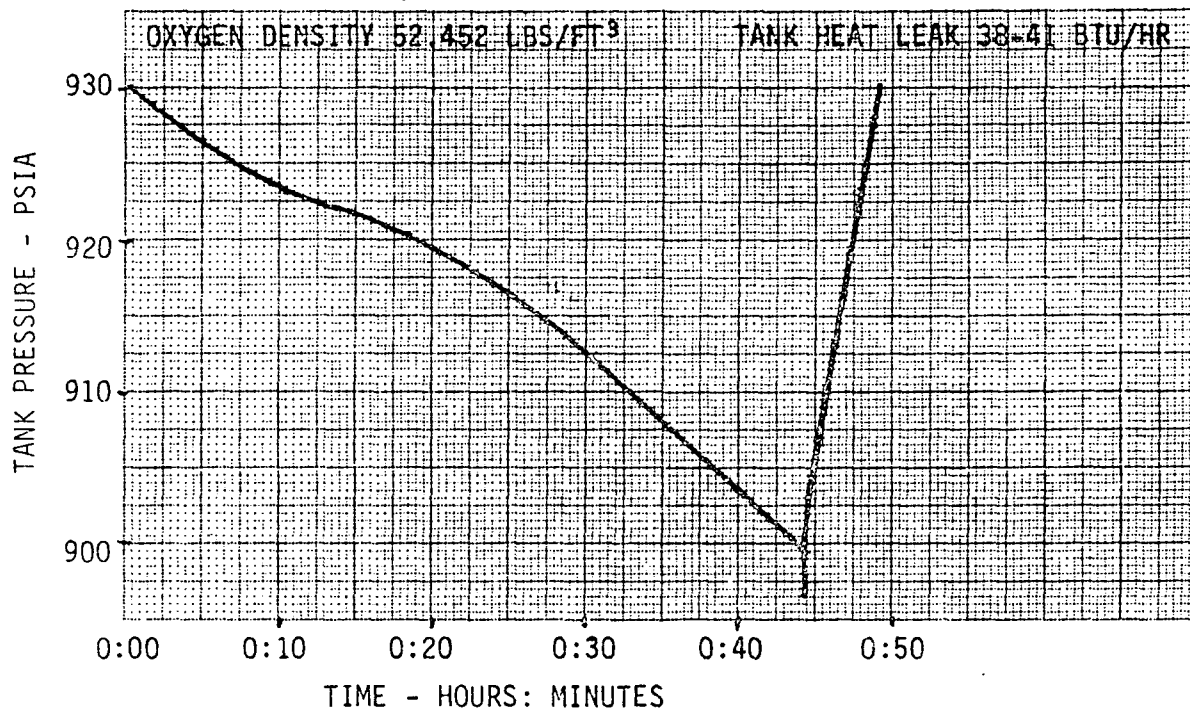| Line Radiation Absorptance	Line Thermal Mass Btu/°R	Total Loop Thermal Mass Btu/°R	Maximum Potential Pressure Decay-PSI
.4	.05	.10	21.652
.4	.10	.20	20.848
.4	.15	.30	19.562
.6	.10	.20	21.626
.2	.10	.20	1.333

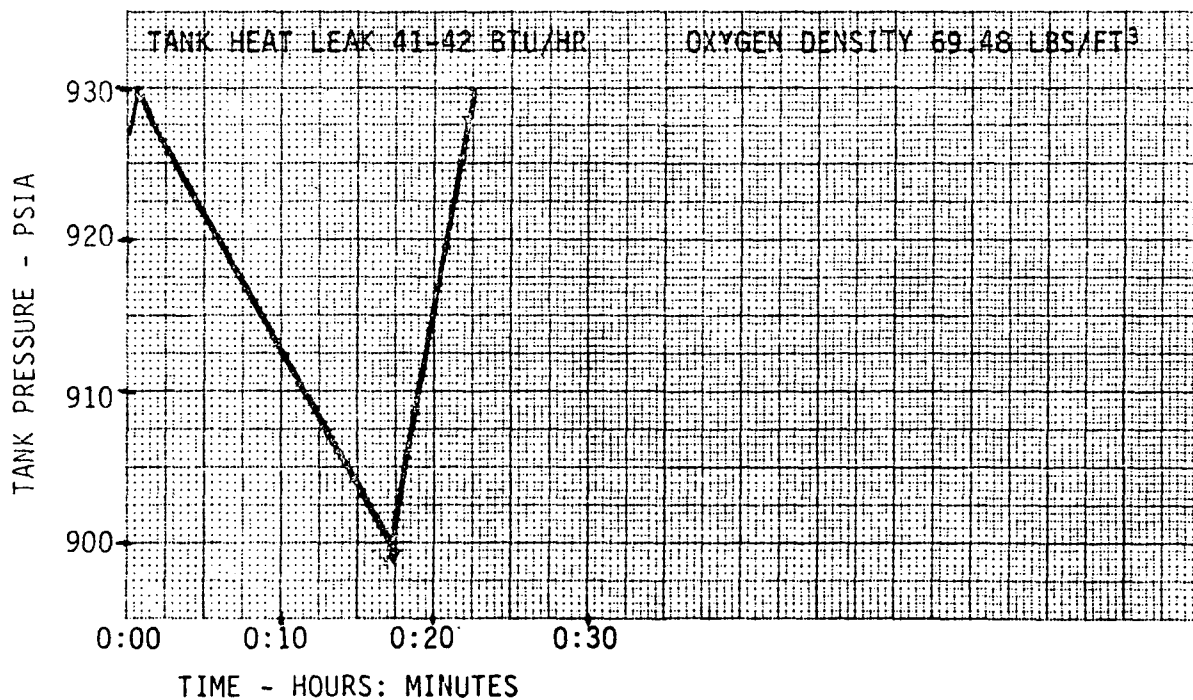FIGURE 3-23. TYPICAL OXYGEN SYSTEM PERFORMANCE,
75% QUANTITY

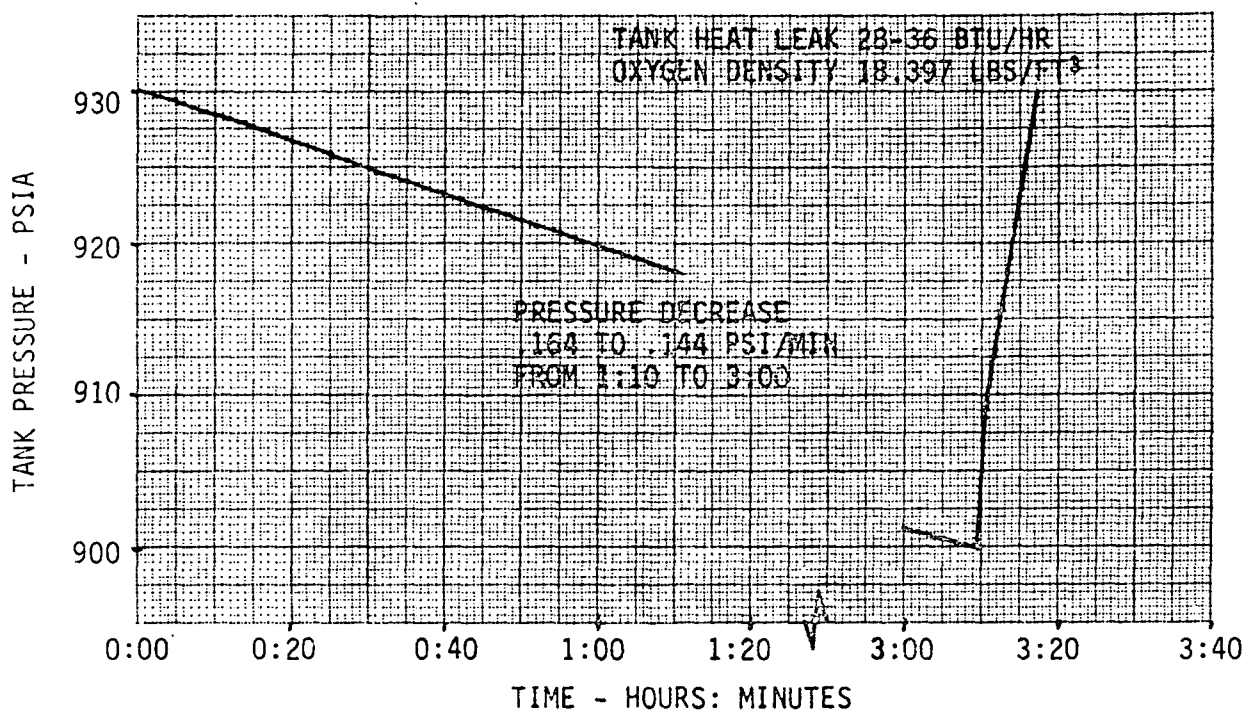FIGURE 3-22. TYPICAL OXYGEN SYSTEM PERFORMANCE,
100% QUANTITY

FIGURE 3-25. TYPICAL OXYGEN SYSTEM PERFORMANCE,
25% QUANTITY
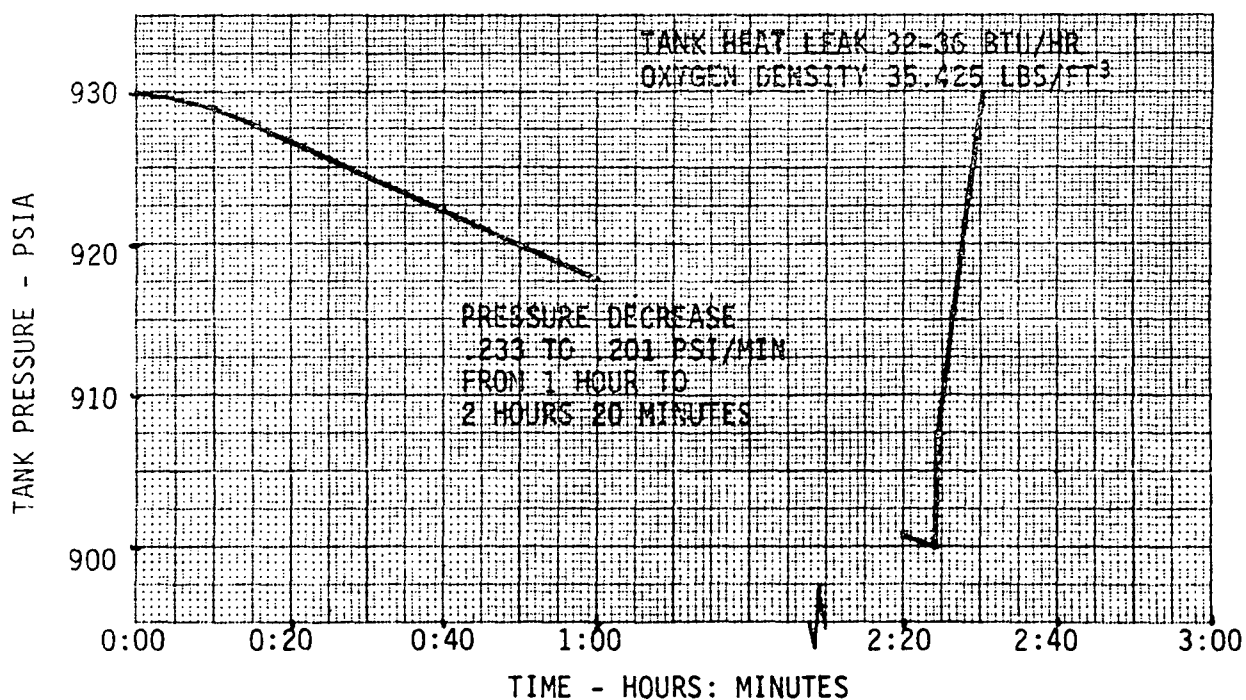
FIGURE 3-24. TYPICAL OXYGEN SYSTEM PERFORMANCE,
50% QUANTITY
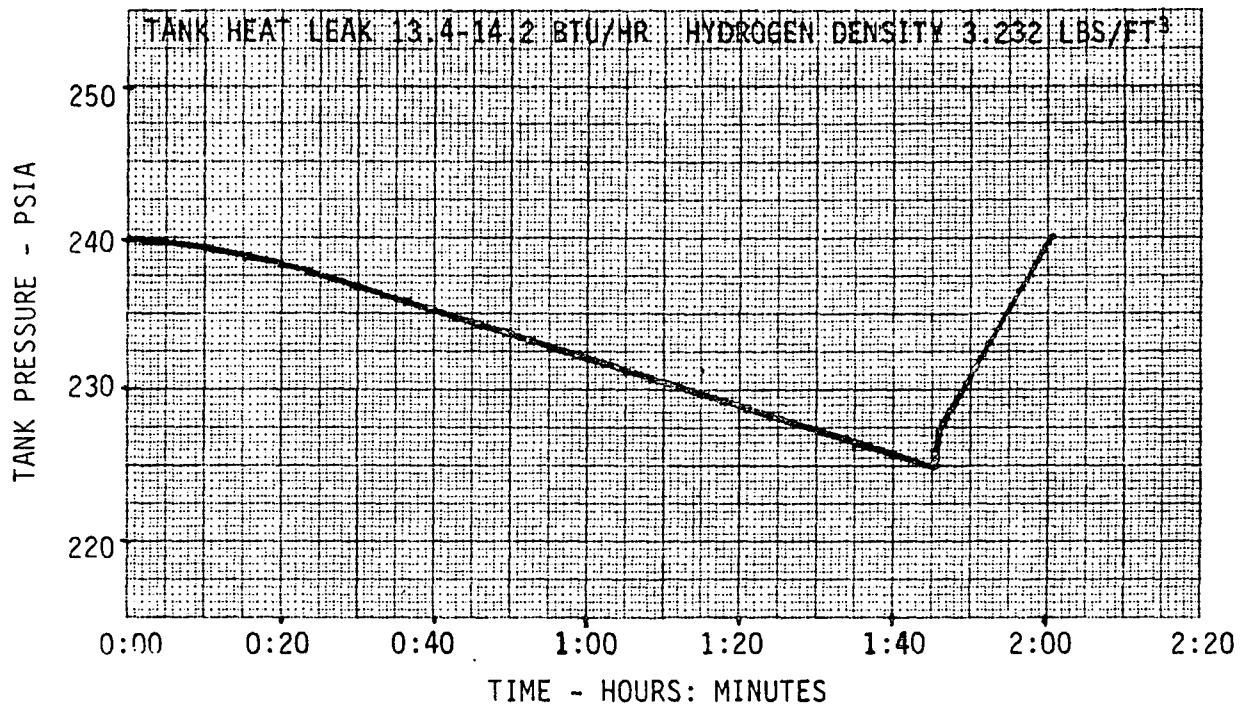
FIGURE 3-27. TYPICAL HYDROGEN SYSTEM PERFORMANCE,
75% QUANTITY
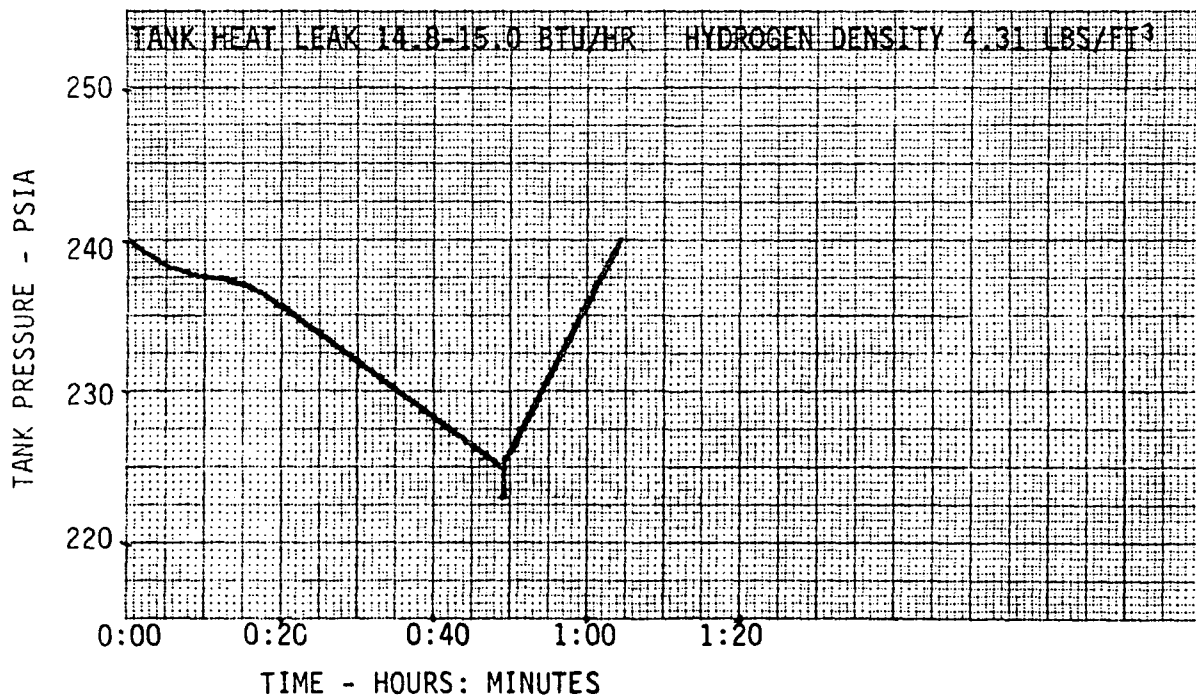
FIGURE 3-26. TYPICAL HYDROGEN SYSTEM PERFORMANCE,
100% QUANTITY

TANK HEAT LEAK 13.3-14.9 BTU/HR   HYDROGEN DENSITY 1.077 LBS/FT³

PRESSURE DECREASE
.061 PSI/MIN
FROM 1 HOUR
TO 4 HOURS
27 MINUTES

TIME - HOURS: MINUTES
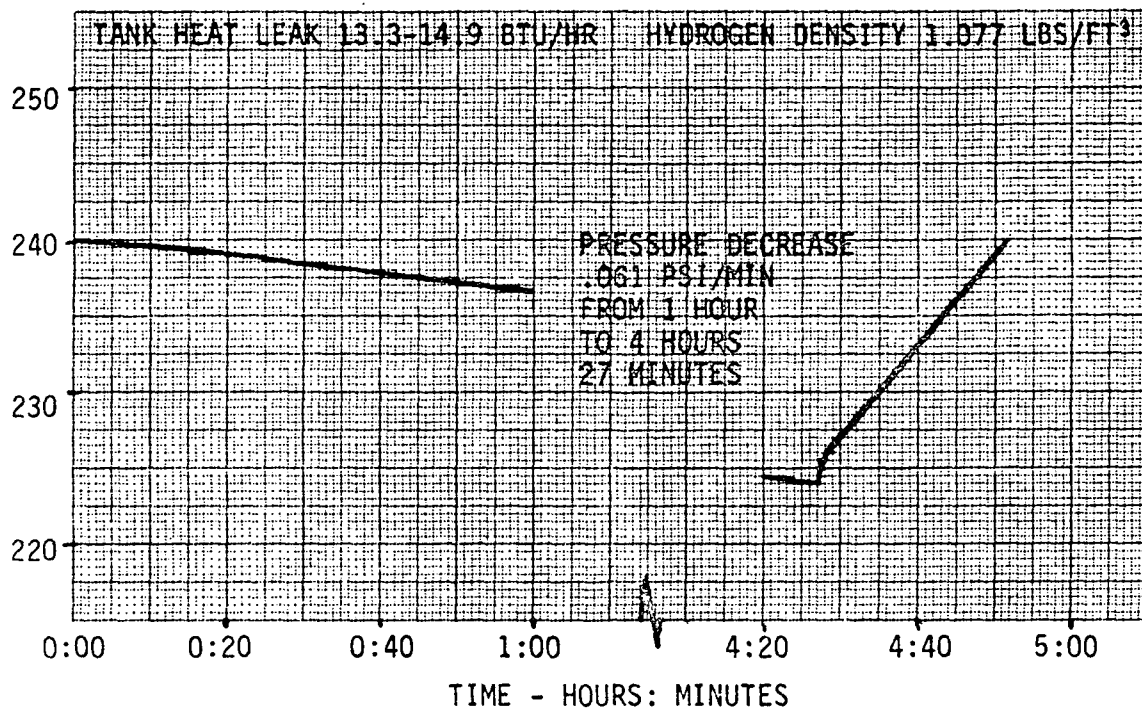
FIGURE 3-29. TYPICAL HYDROGEN SYSTEM PERFORMANCE,
25% QUANTITY

TANK HEAT LEAK 9.6-14.3 BTU/HR   HYDROGEN DENSITY 2.156 LBS/FT³

PRESSURE DECREASE
.056 PSI/MIN
FROM 1 HOUR
TO 4 HOURS
52 MINUTES

TIME - HOURS: MINUTES

FIGURE 3-28. TYPICAL HYDROGEN SYSTEM PERFORMANCE,
50% QUANTITY

3.3.3 <u>Combined Potential Pressure Decay Results</u> (continued)

These data indicate that the loop thermal mass does not significantly affect the pressure decay. Line heating resulting from radiation absorption strongly affec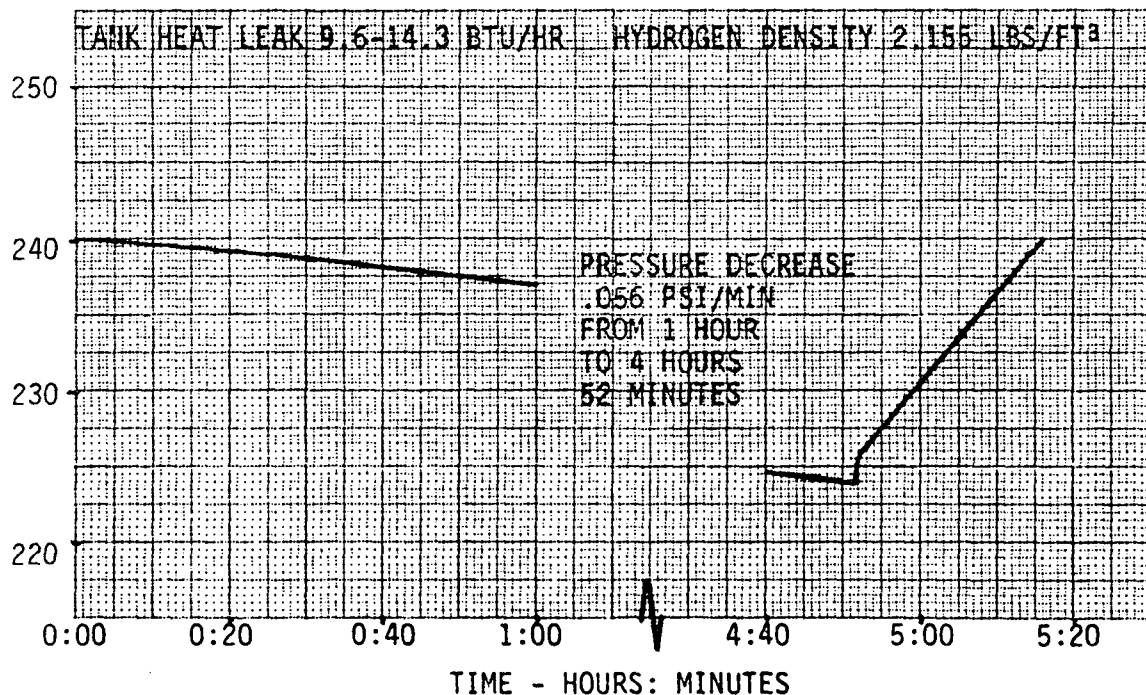ted the pressure decay as the absorptance coefficient was varied from .2 to .4. The potential pressure decay can therefore be limited by insulating the line from the environment.

Hydrogen simulations conducted at a loop-to-tank volume ratio of .0003 and worst case conditions of density (4.30 lbs/ft^3) and flow rate (.16 lbs/hr) resulted in potential pressure decays shown by the table below.

Line Radiation Absorptance	Line Thermal Mass Btu/°R	Total Loop Thermal Mass Btu/°R	Maximum Potential Pressure Decay-PSI
.1 & .2	.01	.02	2.182
	.05	.10	2.174

The hydrogen potential pressure decay results were essentially identical for the range of loop heating and thermal mass values investigated. These results indicate that the hydrogen loop absorptance must be less than .1 to reduce the pressure decay. The potential pressure decay values obtained were, however, well within the tolerable range.

SECTION 4

4.0 CONCLUSIONS

Conclusions drawn from the analysis of the Shuttle supercritical cryogenic tanks with external pressurization systems were:

a. The tank pressure can be adequately controlled if the loop-to-tank volume ratio and the loop thermal mass are small.

b. The tank acceleration level, the fluid injection velocity, and the pump acceleration characteristics do not significantly affect the system performance.

c. Some small pressure overshoot will occur for the hydrogen system unless the loop is insulated.

d. Pressure overshoot will not occur for the oxygen system unless environmental loop heating is greater than that obtained from radiation only.

e. The system potential pressure decay is directly proportional to the loop volume.

f. The fluid contained within the tank will not develop significant temperature stratification or contribute to the system potential pressure decay.

g. The computer program developed to analyze the external loop pressurization system is adequate for predicting pressure transients.

SECTION 5

5.0 RECOMMENDATIONS

The volume and thermal mass of the external loop should be as small as possible to minimize pressure excursions outside the control band. The computer program developed for this analysis should be verified by comparing simulation results with external loop experimental data when available. A simplified computer program should be developed to analyze external loop systems based on the assumption that the fluid in the tank and each line is isothermal but at different temperatures.

APPENDIX A

TANK AND SYSTEM DESCRIPTION

Baseline tank and system data were selected to approximately represent the expected Shuttle cryogenic system. Line diameters were assumed larger than expected to reduce computer time requirements. The increased diameter did not significantly affect the system performance. The baseline data used for the analysis are summarized below.

	Assumed Parameter Value	
Parameter	Oxygen System	Hydrogen System
Tank		
Radius - in.	19.5	21.6
Volume - ft^3	18	24.85
Wall thickness - in.	.092	.068
Heat leak - Btu/hr	44	15
Young's Modulus - psi	3×10^7	1.7×10^7
Poisson's Ratio	.29	.30
Loop		
Line to pump		
Diameter - in.	1.16	1.16
Length - in.	74.3	74.3
Surface area - ft^2	.7293	.7293
Thermal mass - Btu/°R	.1	.01
Radiation Absorptance	.4	.1
Volume - ft^3	.004554	.004554
Line from pump		
Diameter - in.	1.16	1.16
Length - in.	45	45
Surface area - ft^2	.7293	.7293
Thermal mass - Btu/°R	.1	.01
Radiation Absorptance	.4	.1
Volume - ft^3	.00276	.00276
Heater		
Length - in.	15	15
Power - Btu/hr	1362	214.83

APPENDIX B

SIMPLIFIED PRESSURE OVERSHOOT/UNDERSHOOT ANALYSIS

A simplified analysis was developed from equilibrium equations to determine the effect of external loop volume and fluid density on potential pressure overshoot/undershoot. The tank and external loop were mathematically represented as a volume with the tank fluid and loop fluid separated by a movable impermeable membrane as shown below. While no fluid can cross the membrane, heat can. Thus, if the loop fluid is initially at a higher temperature than the tank fluid, heat will flow from the loop to the tank fluid until equilibrium conditions are obtained.
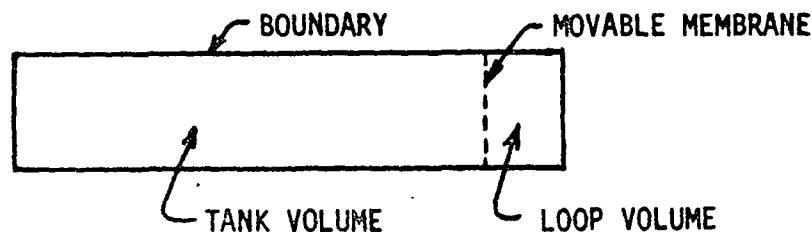
SIMPLIFIED TANK MODEL FOR EQUILIBRIUM ANALYSIS

The pressure change in each portion of the volume can be found from equilibrium thermodynamics as follows:

$$dP_T = \frac{\phi_T}{V_T} (dQ_T + \theta_T dm_T) - \frac{dV_T}{V_T} \rho_T \theta_T \phi_T \tag{1}$$

$$dP_L = \frac{\phi_L}{V_L} (dQ_L + \theta_L dm_L) - \frac{dV_L}{V_L} \rho_L \theta_L \phi_L \tag{2}$$

where

T = Indicates a tank fluid property
L = Implies a loop fluid property
dP = Pressure change (psi)
dQ = Heat transfer (Btu)
dm = Mass change (lb)
dV = Volume change (ft^3)
V = Volume (ft^3)
ρ = Fluid density (lb/ft^3)

APPENDIX B (continued)

$$\phi = \frac{1}{\rho} \left(\frac{\partial \rho}{\partial e} \right)_{\rho} \text{(psi-ft}^3/\text{Btu)}$$

$$\theta = -\rho \left(\frac{\partial h}{\partial \rho} \right)_{\rho} \text{(Btu/hr)}$$

The heat transfer across the boundary can be determined from these equations by noting that:

1. $dP_T = dP_L$ Since the boundary is movable, the pressure in the loop and tank are equal.

2. $dm_T = dm_L = 0$ No fluid is allowed to cross the membrane or flow out of the tank.

3. $dQ_T = -dQ_L$ The only heat transfer is across the membrane.

4. $dV_T = -dV_L$ The total volume does not change.

Therefore, solving equations (1) and (2) for the heat transfer

$$dQ_L = \frac{dV_L}{\frac{\phi_L}{V_L} + \frac{\phi_T}{V_T}} \left(\frac{\rho_T \phi_T \theta_T}{V_T} + \frac{\rho_L \phi_L \theta_L}{V_L} \right) \tag{3}$$

The pressure change due to this heat transfer can be found from either equilibrium equations (1) or (2). Substituting equation (3) into equation (2) and simplifying, the pressure change in the loop and tank is

$$dP = \frac{dV_L}{V_L} \left[\frac{\rho_L \phi_L \theta_L + \frac{V_L}{V_T} \rho_T \phi_T \theta_T}{1 + \frac{V_L}{V_T} \frac{\phi_T}{\phi_L}} - \rho_L \theta_L \phi_L \right] \tag{4}$$

Defining the final equilibrium state with the subscript "F", the change in loop volume is

$$dV_L = V_L - V_{LF}$$

APPENDIX B (continued)

At equilibrium, the loop and tank densities are equal. Therefore,

$$\rho_{LF} = \frac{\rho_L V_L + \rho_T V_T}{V_T + V_L}$$

and

$$dV_L = V_L - \frac{\rho_L V_L}{\rho_L V_L + \rho_T V_T}(V_T + V_L)$$

$$dV_L = V_L\left(1 - \frac{1 + \frac{V_L}{V_T}}{\frac{\rho_T}{\rho_L} + \frac{V_L}{V_T}}\right)$$

Thus, potential pressure overshoot/undershoot can be calculated from the following equation:

$$dP = \left(1 - \frac{1 + \frac{V_L}{V_T}}{\frac{\rho_T}{\rho_L} + \frac{V_L}{V_T}}\right)\left[\frac{\rho_L \phi_L \theta_L + \frac{V_L}{V_T}\rho_T \phi_T \theta_T}{1 + \frac{V_L}{V_T}\frac{\phi_T}{\phi_L}} - \rho_L \phi_L \theta_L\right]$$

Comparison of the pressure change associated with loop/tank volume ratios of .0005 to .002 indicated that the pressure change was proportional to the volume ratio $\left(\frac{V_L}{V_T}\right)$. For small loop/tank volume ratios, the pressure change can therefore be computed from

$$dP = \left(\frac{dP}{V_L/V_T}\right)\frac{V_L}{V_T}$$

The quantity $\frac{dP}{V_L/V_T}$ may be evaluated at any small convenient volume ratio.